X-551-71-246
PREPRINT

ANALYSIS OF MINITRACK RESIDUALS

B. ROSENBAUM

DECEMBER 1970

GSFC
GODDARD SPACE FLIGHT CENTER
GREENBELT, MARYLAND

X-551-71-246
PREPRINT

ANALYSIS OF MINITRACK RESIDUALS

by
B. Rosenbaum

December 1970

Goddard Space Flight Center
Greenbelt, Maryland

ANALYSIS OF MINITRACK RESIDUALS

by
B. Rosenbaum
Goddard Space Flight Center

ABSTRACT

An analysis is given on Minitrack residuals for the tracking of GEOS-I. The data stem from previous calculations by Marsh et al. (1970) under the Minitrack-optical tracking intercomparison program. The intent of the present study is to evaluate bias and systematic effects imbedded in the residuals. The treatment of the ionospheric refraction is eased since the tracking observations are during the nighttime and late afternoon and the period is during the minimum of the solar sunspot number. A finding of the analysis is that the direction cosine residuals exhibit a linear bias versus the Minitrack angles (α for the polar mode and β for the equatorial mode). The bias parameters are a function of the direction cosine as well as the station and tracking mode. The residual noise (residuals corrected for ionsopheric refraction and the linear bias) is 8.5×10^{-5} for which systematic effects are a significant contributing component. We estimate the uncorrelated rms noise to be 4×10^{-5}. This is attributed mainly to instrumental noise of 2×10^{-5} corresponding to the quantization step for phase difference measurement; and ionospheric refractive noise estimated at 3×10^{-5} for an ionosphere and elevation angle representative of the test data. At several sites the residual noise is 5×10^{-5} for either the equatorial or polar tracking mode.

CONTENTS

ANALYSIS OF MINITRACK RESIDUALS

by
B. Rosenbaum
Goddard Space Flight Center

INTRODUCTION

An objective of the GEOS-I program has been to utilize the satellite to calibrate tracking equipment and evaluate system tracking accuracies. During the program many tracking systems using radio or optical methods participated in the tracking of the satellite. This report is a study of bias and noise in Minitrack direction cosine residuals for the tracking of GEOS-I. The residuals are a result of the Minitrack-optical tracking intercompar'son by Marsh et al. (Ref. 1). The data stem from observations covering 5 1/4 days from December 31, 1965 to January 5, 1966. The satellite was in an elliptical orbit with approximate orbital parameters: altitude of the perigee, 1,100 km; altitude of the apogee, 2,300 km; and an orbital plane inclination, 59.4°. The orbital period was 2.005 hours.

As a reference for evaluating the accuracy of Minitrack observations Marsh et al. employed a standard reference orbit for GEOS-I determined from very precise optical tracking data. The calculation of the standard orbit was based on the SAO M-1 Earth gravitational model (Ref. 2) which had been modified to incorporate the significant harmonic terms that are resonant in the GEOS-I orbit. Station location datums were transformed to the SAO C-5 standard Earth model. A measure of the precision of the reference orbit is the rms residual deviation of the optical observations which amounted to 3 arc seconds. This compares favorably with 2 arc seconds given as the precision of the optical tracking.

Minitrack observations were compared with predictions of the reference orbit. The rms of the residuals is 1.9×10^{-4} which exceeds the nominal Minitrack accuracy of 1×10^{-4} by nearly a factor of two. The discrepancy has been attributed by the investigators primarily to station systematic bias and ionospheric refraction.

The intent of the present work is to determine the perturbations introduced by the ionosphere and to evaluate the station biases and the residual noise factor. Various systematic effects are also shown to be imbedded in the residual noise. The results are considered to be applicable to the Minitrack calibration procedure (Berbert, et al., Ref. 26).

DIRECTION COSINE RESIDUALS

During tracking operations the Minitrack stations measure the direction cosines (ℓ, m) of the arrival direction of the satellite signal using a crossed pair of interferometers. At the sites there

are two independent tracking modes designated as polar and equatorial having fan-shaped antenna beams oriented east-west and north-south, respectively. Each mode has its own crossed interferometers. In Figure 1, the two modes are shown as spatially separated for the sake of clarity, although their electrical centers (c) actually coincide. Tracking is performed when the satellite is within an antenna beam. The mode which tracks will depend on the direction of the trajectory and the zenith angle at closest approach.

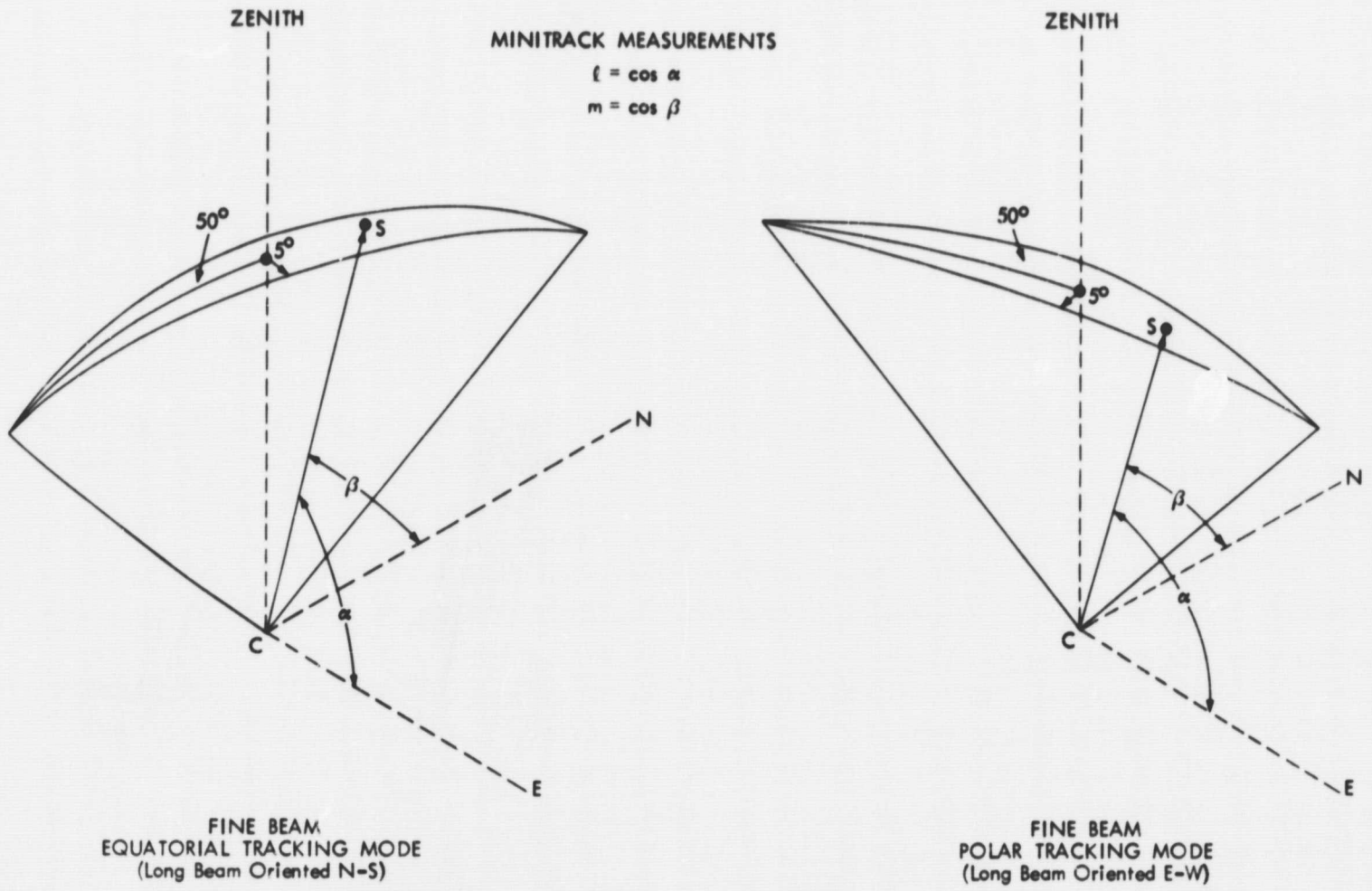

Figure 1 - Approximate reception pattern of the fine beam of the 136 MHz Minitrack antenna array (after Marsh, et al., Ref. 1).

When a satellite traverses one of the antenna beams the system makes a series of phase difference measurements. The output data (ℓ, m) are deduced from a smooth polynomial fit to the observations. There may be from one to three cosine pairs generated from a single set of observations. The multiples are not suited for the purposes of our analysis since they are correlated and their redundancy gives uneven statistical weight to a set of tracking observations. In order to have the observation set represented by a single residual pair ($\Delta\ell$, Δm) we adopt the procedure of contracting a multiple to a single pair by taking an average value over the multiple. The data so treated are a small fraction of the total data and are summarized in Table 1. Those data in brackets were previously rejected by Marsh et al. because the residuals were large, greater than 5×10^{-4}. Consistent with these investigators we have adopted a similar procedure of

Table 1

Contraction of Multiple Residual Pairs ($\Delta\ell$, Δm)

Tracking Station	Mode	Residual				Average Residual			
		$\Delta\ell \times 10^3$	$\Delta m \times 10^3$	α	β	$\Delta\ell \times 10^3$	$\Delta m \times 10^3$	α	β
Blossom Point	Equatorial	.053	-.221		50.3	-.049	-.256		48.5
		-.079	-.269		48.4				
		-.120	-.279		46.7				
	Equatorial	.058	-.180		38.4	.041	-.196		37.4
		.024	-.211		36.3				
	Polar	.011	-.101	151.1		-.001	-.096	150.4	
		-.013	-.090	149.6					
Fort Myers	Polar	.088	-.349	95.8		.071	-.320	94.7	
		.054	-.291	93.6					
E. Grand Forks	Equatorial	.085	-.050		52.6	.057	-.060		51.7
		.028	-.069		50.8				
	Polar	.059	.134	128.6		.071	.119	127.0	
		.083	.103	125.3					
Lima	Polar	.102	-.092	73.2		.141	-.061	72.2	
		.112	-.096	72.9					
		.210	.005	70.6					
Mojave	Polar	.371	-.138	128.1		.379	-.129	126.8	
		.387	-.119	125.5					
	Polar	-.12	[5.4]	34		Rejected			
		.150	-.155	30.8					
	Equatorial	.302	.001		119.7	.320	.042		118.1
		.337	.083		116.4				
	Equatorial	.015	-.086		19.8	.046	-.133		19.4
		.077	-.179		19.0				
	Equatorial	.022	-.190		18.1	-.065	-.203		17.9
		-.151	-.215		17.7				
	Equatorial	(-.412)	-.405		25.0	-.111	-.277		25.7
		.191	-.149		26.3				
St. John's	Polar	-.450	.083	39.5		-.425	.028	38.9	
		-.418	.061	39.1					
		-.406	-.059	38.0					
	Polar	-.064	.004	85.5		.063	.015	84.0	
		-.067	.007	84.5					
		-.057	.034	82.0					
	Equatorial	.023	.002		103.9	-.020	.014		100.7
		-.062	.026		97.4				
Winkfield	Equatorial	.176	-.145		59.5	Rejected			
		[187.9	47.9]		61				
	Equatorial	[132.	113.]		111	Rejected			
		.248	.062		103				
		.202	-.047		100				

A bracket denotes a point rejected by Marsh et al. (Ref. 1)

A parenthesis denotes a point rejected in the linear regression analysis.

Table 2

Summary of Number of Residual Pairs ($\Delta\ell, \Delta m$)

Tracking Station	Observations	Decrease from contraction See Table 1		Observations in Figure 2		Rejected for exceeding 3×10^{-4} criterion		ν Observations in regression analysis	
		Polar	Equatorial	Polar	Equatorial	Polar	Equatorial	Polar	Equatorial
Blossom Point	46	1	3	17	25		2	17	23
College	21				17		2	*	15
East Grand Forks	27	1	1	8	17	2		6	17
Fort Myers	17		1	11	5	1		10	5
Johannesburg	2							*	*
Lima	7	2						*	*
Mojave	36	2	4	11	19		2	11	17
Quito	4							*	*
St. John's	36	4	1	10	21			10	21
Santiago	4							*	*
Winkfield	16		4		10			*	10
Woomera	4							*	*
Total	220	10	14	57	114	3	6	54	108

*Station modes not subjected to linear regression analysis.
Modes having less than five data points do not appear in Figure 2.

rejecting an entire multiple if one of its members exceeded the same criterion. This resulted in the rejection of three groups (one for Mojave and two for Winkfield). One more group is also rejected in the regression analysis as described below.

Linear regression analysis. Tracking operations are normally confined to zenith angles less than 50°. For the current test data the acquisitions were extended to zenith angles of 75°. In this study we find that the residuals have a bias relationship with respect to the Minitrack angle measured from the baseline of the antenna beam. Accordingly Figure 2 shows the residuals (from Ref. 1) versus the angle α ($\ell = \cos\alpha$) for the polar mode and β ($m = \cos\beta$) for the equatorial mode. Twelve Minitrack stations are represented in the test data, but the bulk of the data is at the seven stations of the northern hemisphere (in part due to predetermined tracking assignments). Only the latter seven stations are shown in Figure 2. The residuals are seen to conform to a linear bias trend and have a scatter with respect to the bias on the order of 1×10^{-4}.

It should be noted that at small zenith angles we are uncertain of the tracking mode. These points are labeled as having an uncertain tracking mode. We have followed a rule of assigning the polar mode when $|m| < |\ell|$ and the equatorial mode when $|\ell| < |m|$. This is consistent with the case of larger zenith angles. The number of points of uncertain tracking mode is 5 percent of the data.

For a residual deviation from the regression line greater than 3×10^{-4} (that is, three times the nominal Minitrack accuracy) we have rejected the residual and its pair. In one case (Mojave, equatorial) a multiple appearing in Table 1 is rejected because one of its members exceeded this criterion. Table 2 gives a summary of the number of residuals by station and mode. The regression analysis has been applied only to those modes having five or more observation points.

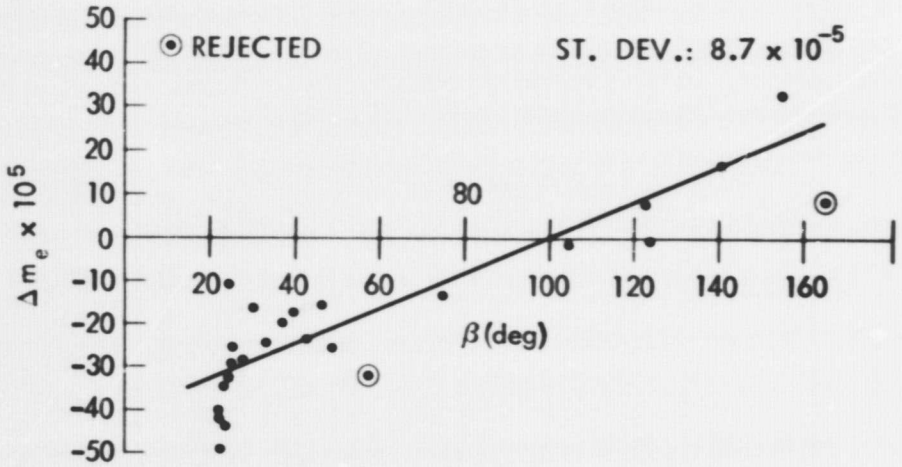

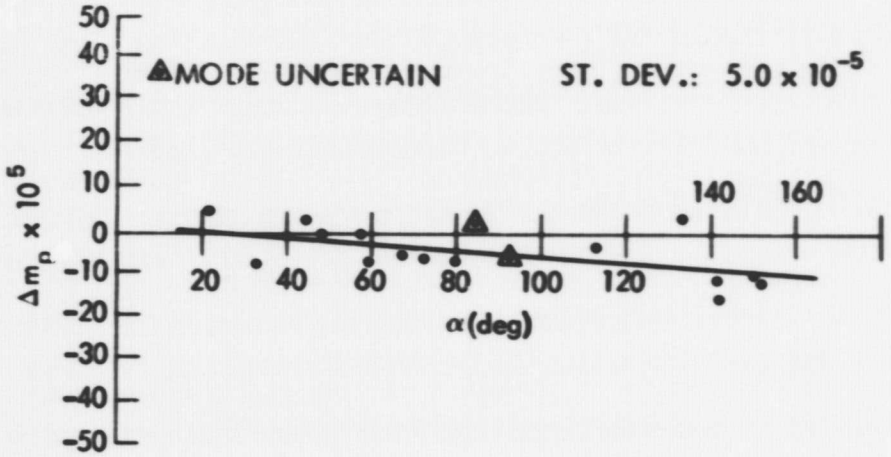

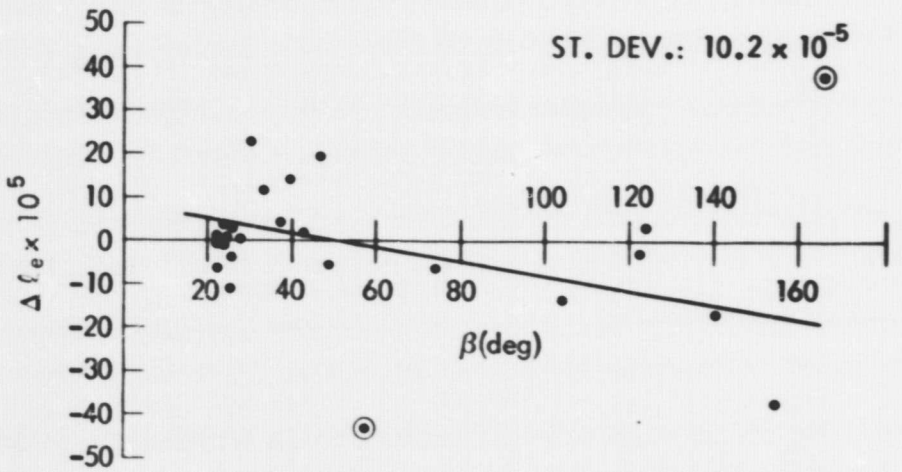

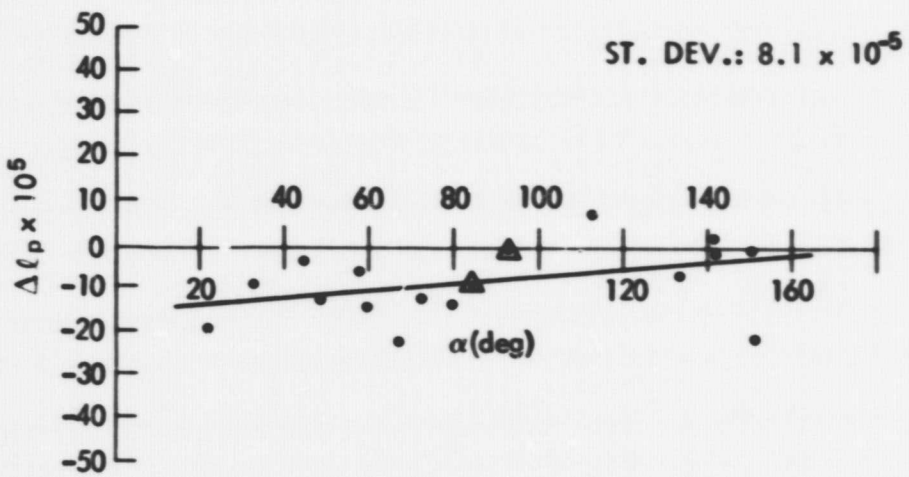

c. Blossom Point, Maryland Equatorial mode
25 observations

b. Blossom Point, Maryland Polar mode
17 observations

Figure 2 - Direction cosine residual (uncorrected) x 10^5 vs. Minitrack angle (α for the polar mode and β for the equatorial mode). The regression line is shown.

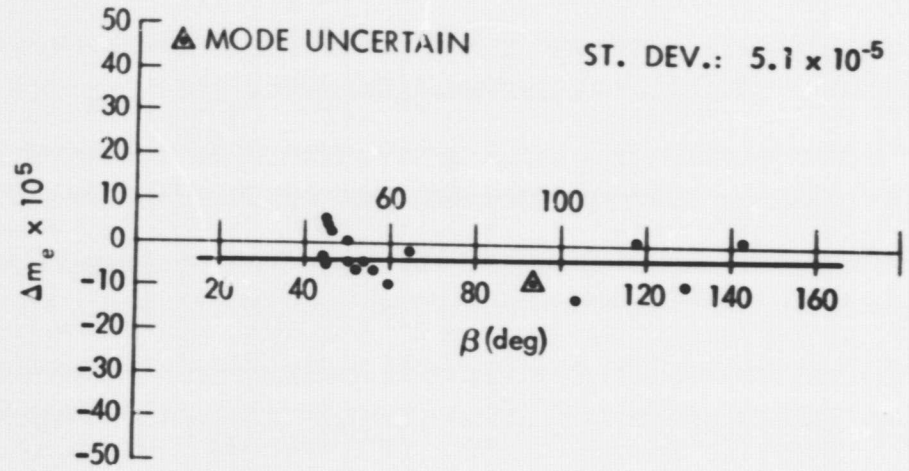

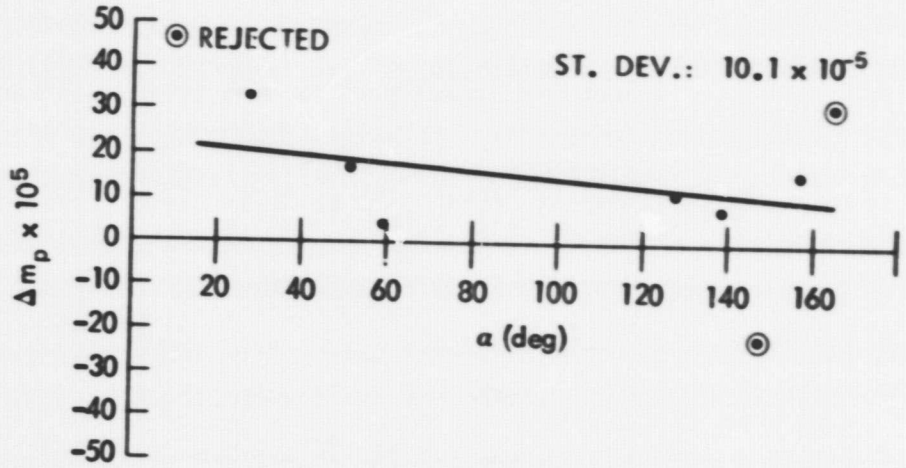

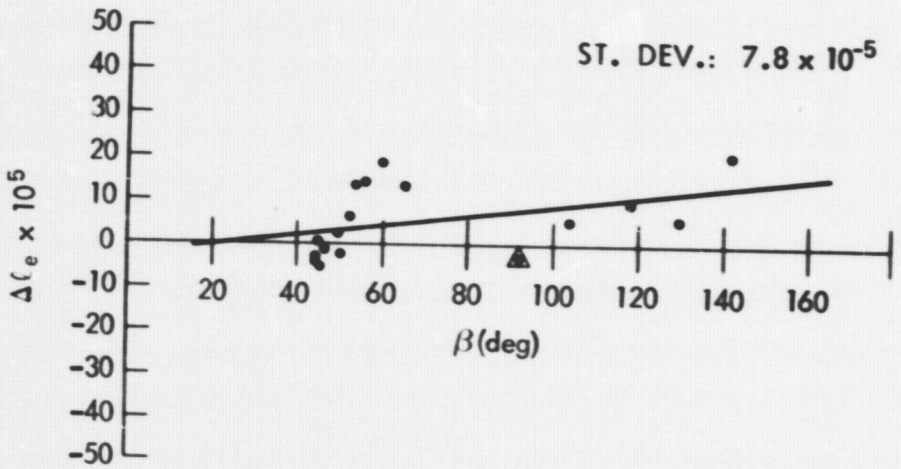

c. East Grand Forks, Minnesota Equatorial mode
17 observations

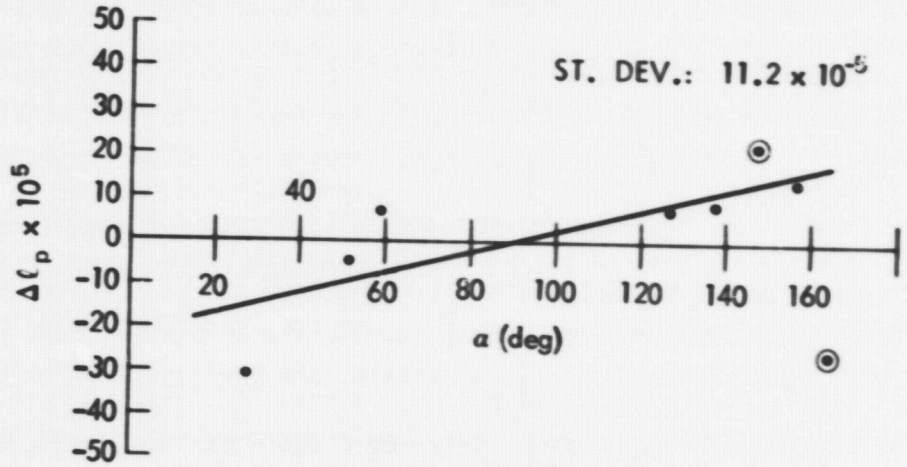

d. East Grand Forks, Minnesota Polar mode
8 observations

Figure 2 - Direction cosine residual (uncorrected) $\times 10^5$ vs. Minitrack angle (α for the polar mode and β for the equatorial mode). The regression line is shown.

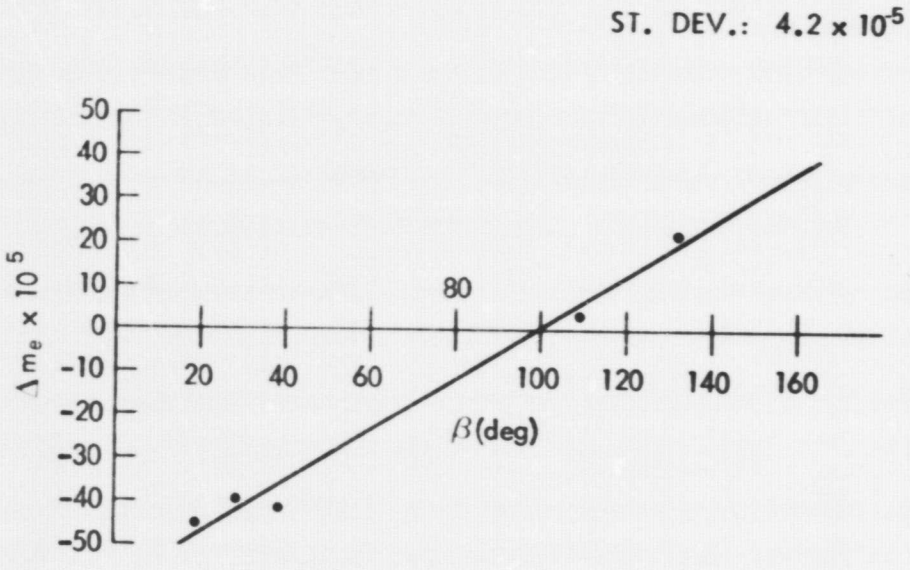

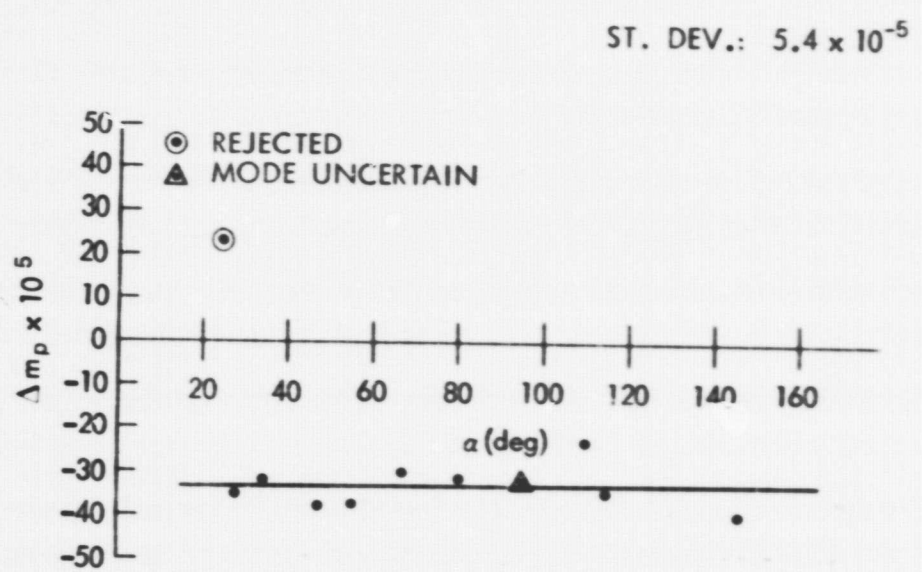

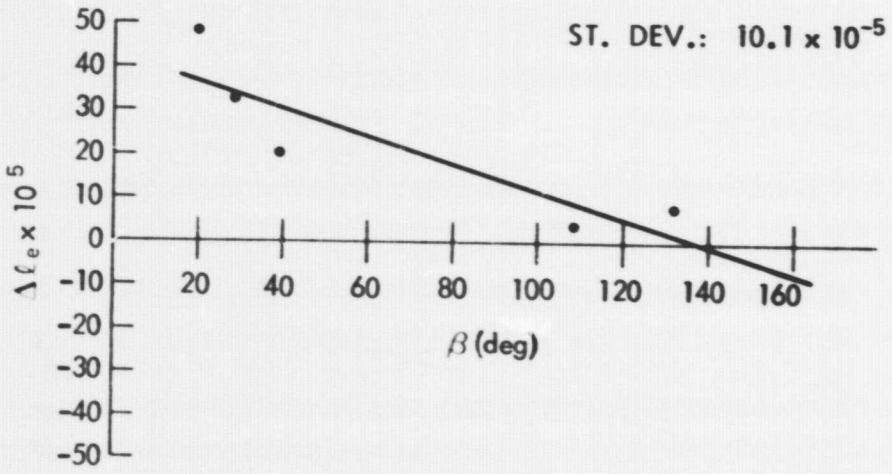

e. Fort Myers, Florida Equatorial mode
5 observations

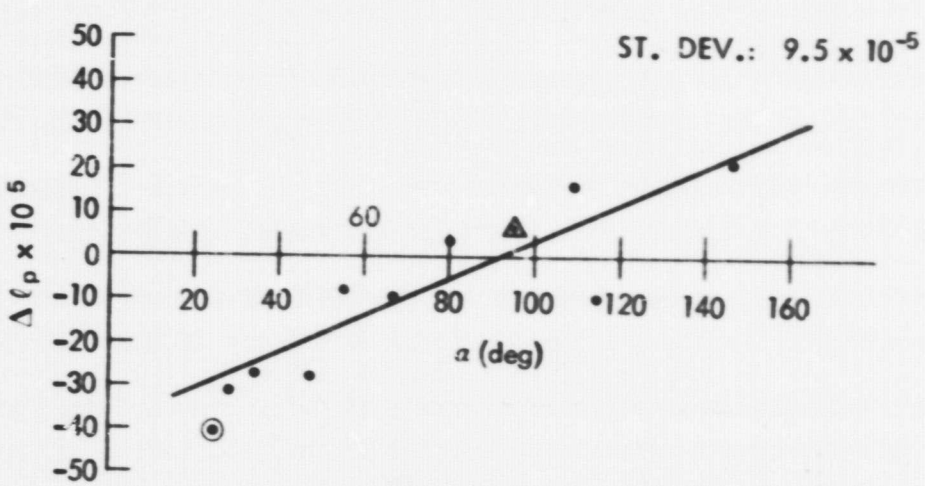

f. Fort Myers, Florida Polar mode
11 observations

Figure 2 - Direction cosine residual (uncorrected) $\times 10^5$ vs. Minitrack angle (α for the polar mode and β for the equatorial mode). The regression line is shown.

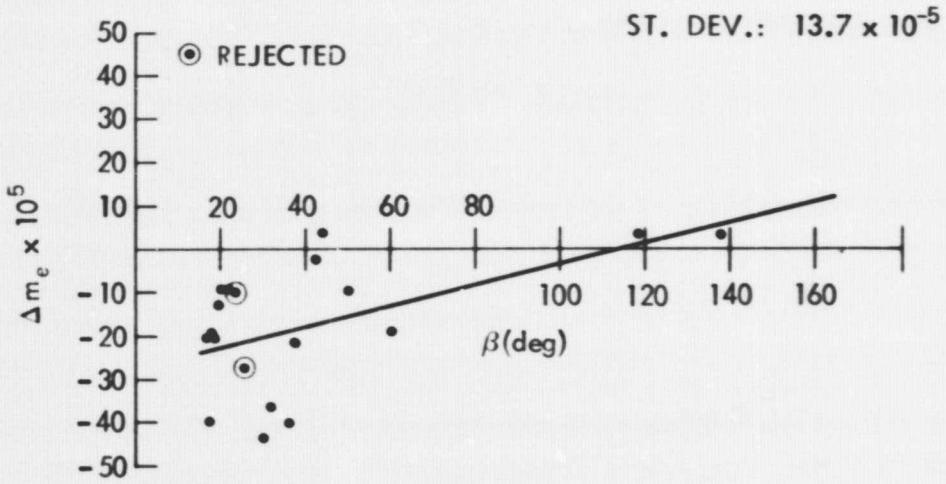

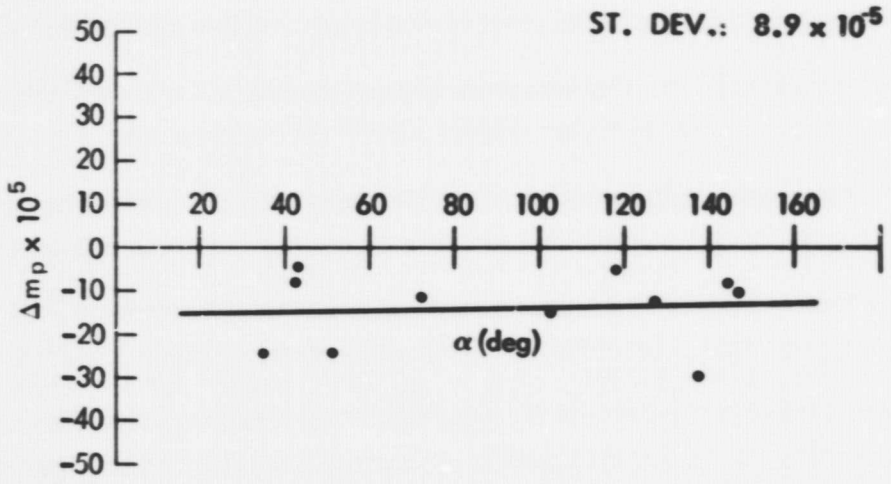

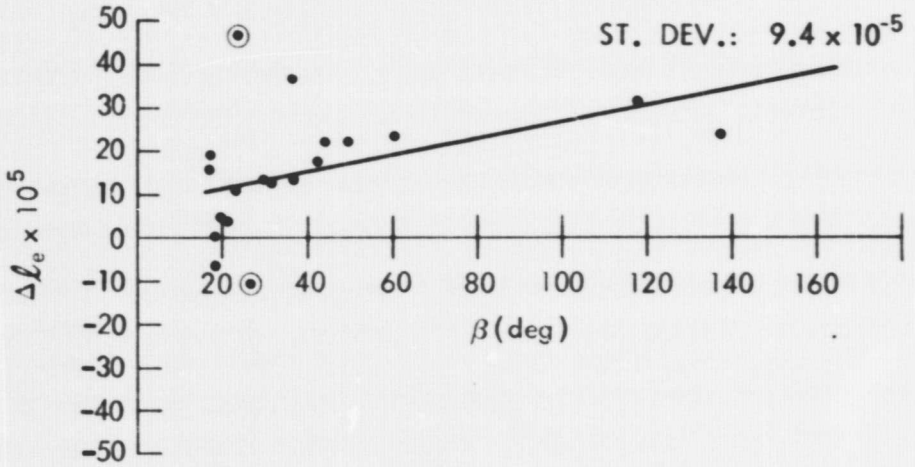

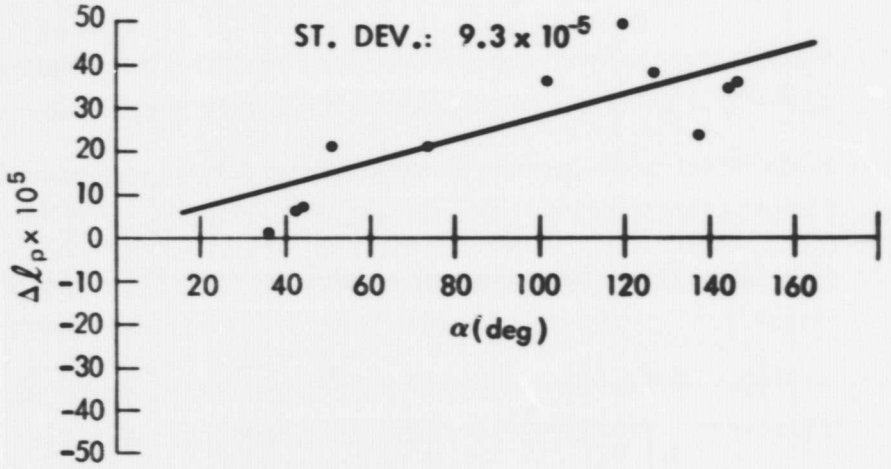

g. Mojave, California Equatorial mode
19 observations

h. Mojave, California Polar mode
11 observations

Figure 2 - Direction cosine residual (uncorrected) $\times 10^5$ vs. Minitrack angle (α for the polar mode and β for the equatorial mode). The regression line is shown.

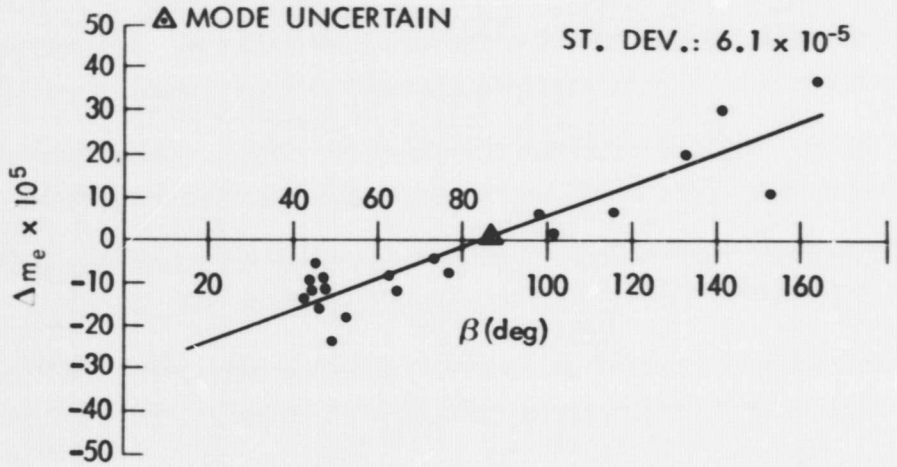

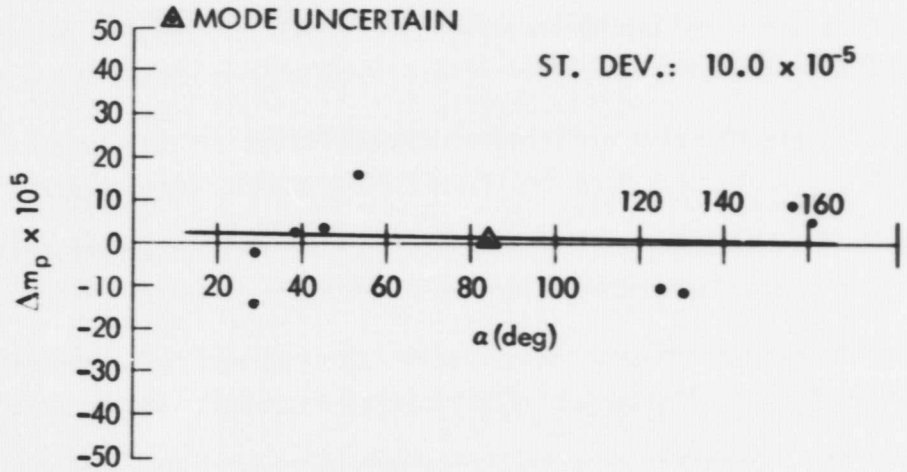

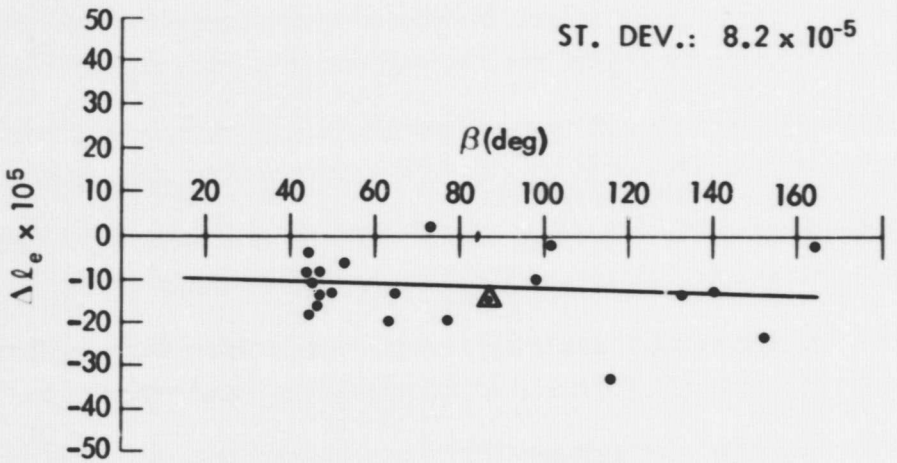

i. St. John's, Newfoundland Equatorial mode
21 observations

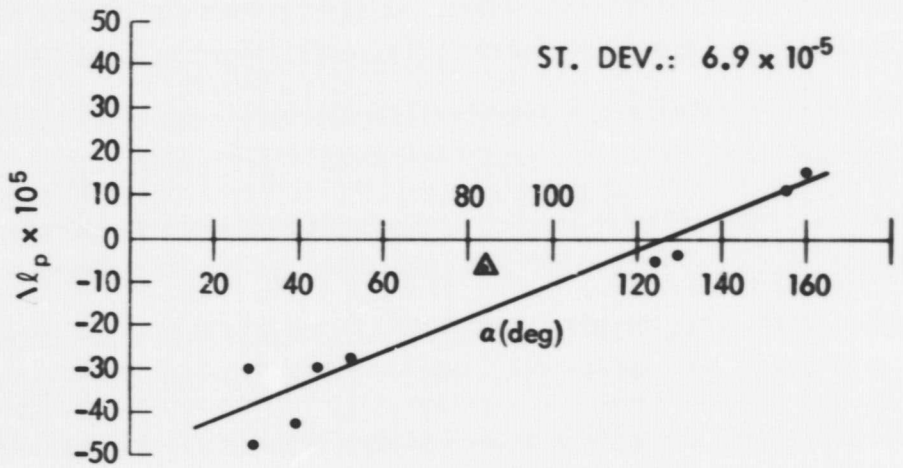

j. St. John's, Newfoundland Polar mode
10 observations

Figure 2 – Direction cosine residual (uncorrected) $\times 10^5$ vs. Minitrack angle (α for the polar mode and β for the equatorial mode). The regression line is shown.

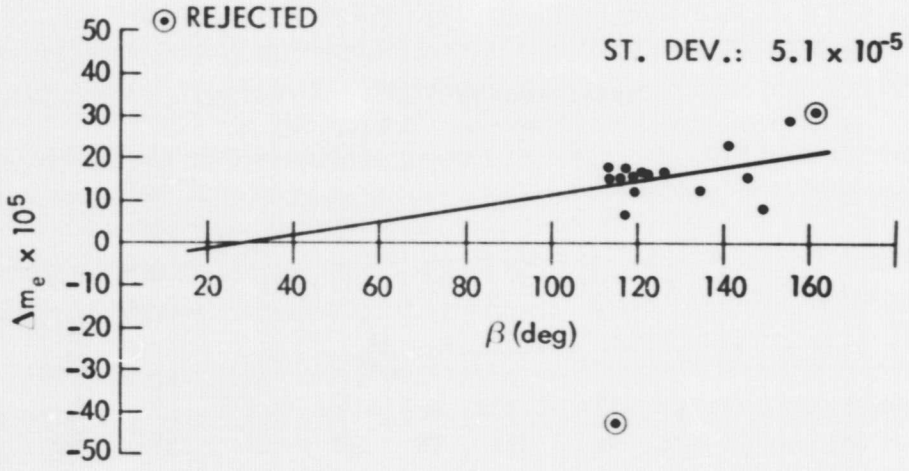

k. College, Alaska Equatorial mode
17 observations

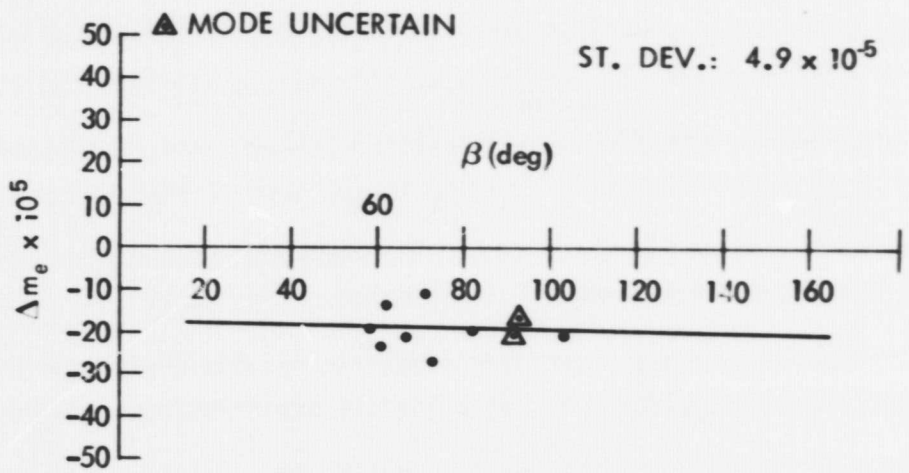

l. Winkfield, England Equatorial mode
10 observations

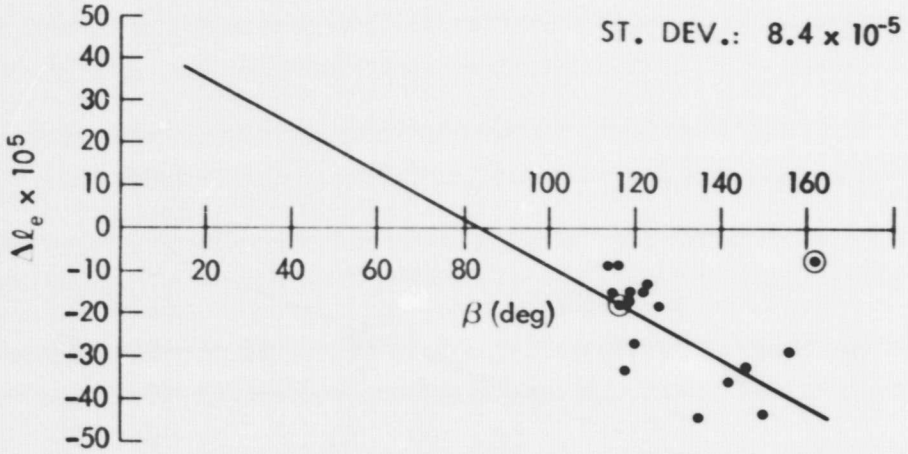

k. College, Alaska Equatorial mode
17 observations

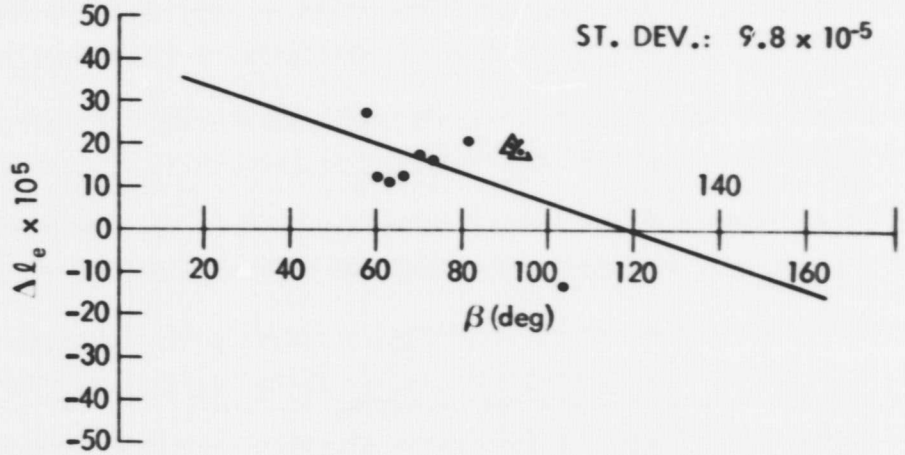

l. Winkfield, England Equatorial mode
10 observations

Figure 2 - Direction cosine residual (uncorrected) $\times 10^5$ vs. Minitrack angle (α for the polar mode and β for the equatorial mode). The regression line is shown.

The regression parameters are z, the zenith bias, and k, the slope bias, while the regression line for the equatorial mode, ℓ residual is

$$\Delta \ell_{e,b} = z_{\ell,e} + k_{\ell,e} (\beta - 90^\circ)$$

and similarly for the three other cases. We calculate the standard deviation with respect to the regression line, $\sigma_{\ell,e}$, by the formula

$$\sigma_{\ell,e} = \sqrt{\frac{\sum_j (\Delta \ell_{e,j} - \Delta \ell_{e,b})^2}{\nu - 2}}$$

where $\Delta \ell_{e,j}$ denotes the residuals, and ν the number of points in the mode.

The magnitudes of the bias parameters and st. dev.'s have a wide range depending on the station, the mode, and the direction cosine. For the polar mode of Fort Myers (Figure 2f) the regression line of the m residuals has a virtually nil slope but a large negative zenith bias, while by contrast the slope for the ℓ residuals is large and the ℓ zenith bias is minimal, -1×10^{-5}. The st. dev. is 9.5×10^{-5} for the ℓ residuals and 5.4×10^{-5} for the m residuals, nearly a factor of two difference. The ℓ and m regression lines for the equatorial mode of the same station (Figure 2e) on the other hand differ markedly from the corresponding lines of the polar mode.

In the equatorial mode of East Grand Forks there are groups of points concentrated in a relatively narrow interval of β between 44° and 64°. The reason is that the satellite period is two hours, so that tracking passes can occur on a near cyclic diurnal basis at similar elevation angles. The points in question are for a series of consecutive orbital tracking passes that repeat diurnally. The feature of the clustered points is that the residuals have a bias-type pattern. In the data those between 44° and 50° have a negative bias and those between 50° and 64° have a positive bias with respect to the regression line.

In the equatorial mode of Blossom Point (Figure 2a) there is as in the previous example a bias effect with respect to the regression line. The data at several other station modes also show evidence of a similar effect. This pattern in the residuals appears as a second order systematic effect superimposed on the main linear bias. There are other aspects of sytematics in the residuals, to be presented in a later section, that appear when the residual noise is exhibited in the time domain.

The residuals in the various tracking modes analyzed have a composite st. dev. with respect to the regression lines of 8.5×10^{-5} which represents a substantial decrease from 19×10^{-5}, the rms of the raw residuals. However, the st. dev. at the various modes show a considerable spread from the composite mean. The maximum st. dev. is on the order of the nominal Minitrack accuracy, while the minimum approaches 4×10^{-5}. The latter is to be associated with the uncorrelated rms residual noise.

The residuals whose properties we have considered here are contaminated by ionospheric refraction. The following section undertakes to treat this problem. Subsequently we reexamine the extent to which correction of ionospheric effects may alter results noted in this section.

IONOSPHERIC REFRACTION

Ionospheric refraction commonly looms as an uncertain, potentially large disturbing factor for Minitrack. In the present data the perturbations are mitigated by several factors. The time period of the data corresponds to the minimum phase of the solar sunspot cycle. Furthermore, the bulk of the tracking was during the local nighttime and the late afternoon ionosphere. Under these conditions the refractive effects are much reduced. However, they are still relevant, especially for tracking which extends down to elevation angles of 15°.

The calculation of the refractive perturbation is based on an ionospheric model which accounts for regular geographic and temporal variations of total electron content, N_t. The day-to-day fluctuations of the medium are not correctable since they can only be compensated if the ionosphere is monitored near the tracking site concurrent with the tracking events. The calculations do incorporate refractive contributions due to horizontal gradients of N_t. Large scale ionospheric irregularities are treated as a source of refractive noise.

Formulas. The refraction of VHF signals in a three dimensionally heterogeneous ionosphere has been studied by Rosenbaum (Ref. 3). The theory shows that for Minitrack the refraction formulas are:

Equatorial mode

$$\Delta \ell_{e,i} = \frac{\eta \sin \alpha}{\cos \lambda_0} \int_0^{R_c} dR \, \frac{(R_c - R)}{R_c} \left(\frac{\partial N_e}{r \, \partial \mu} \right) \tag{1a}$$

$$\Delta m_{e,i} = - \frac{\eta \, r_0 \, r_c}{R_c} \sin \beta \cos \beta \cos \phi_c \int_{r_0}^{r_c} \frac{dr \, N_e}{r^2 \cos^3 \phi} + \eta \sin \beta \int_0^{R_c} \frac{dR}{\cos \phi} \, \frac{(R_c - R)}{R_c} \left(\frac{\partial N_e}{r \, \partial \lambda} \right) \tag{1b}$$

Polar mode

$$\Delta \ell_{p} = - \frac{\eta \, r_0 \, r_c}{R_c} \sin \alpha \cos \alpha \cos \phi_c \int_{r_0}^{r_c} \frac{dr \, N_e}{r^2 \cos^3 \phi} + \frac{\eta \sin \alpha}{\cos \lambda_0} \int_0^{R_c} \frac{dR}{\cos \phi} \, \frac{(R_c - R)}{R_c} \left(\frac{\partial N_e}{r \, \partial \mu} \right) \tag{1c}$$

$$\Delta m_{p,i} = \eta \sin \beta \int_0^{R_c} dR \, \frac{(R_c - R)}{R_c} \left(\frac{\partial N_e}{r \, \partial \lambda} \right) \tag{1d}$$

and

$$r \sin \phi = r_0 \sin \phi_0 = r_c \sin \phi_c \tag{2}$$

where the integrals are taken along the line of sight from the tracking station, o, to the satellite position, c; and

dr = $dR \cos \phi$
r = distance from the Earth center
R = distance along the line of sight from the tracking station toward the satellite
N_e = electron density (m^{-3})
η = 21.8×10^{-16} (m^3), proportionality factor of the refractivity at VHF
$-\eta N_e$ = 10^{-6} × refractivity
λ = latitude
μ = longitude
ϕ = angle formed by the line of sight and the radial line from the Earth center

Figure 3 illustrates the geometry for the equatorial mode. The geometry is similar for the polar mode.

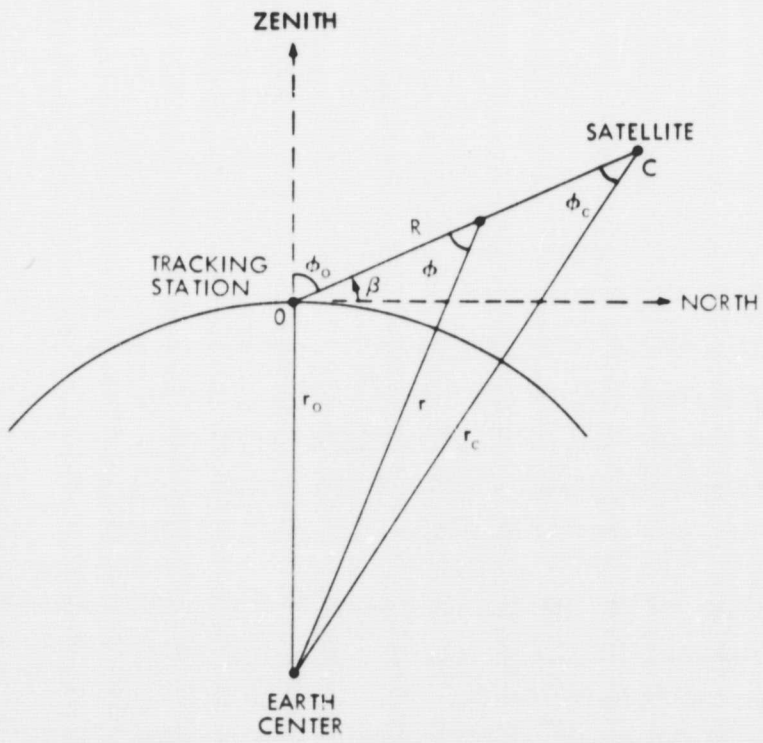

Figure 3 - Geometry for the equatorial mode, meridian plane.

The terms of Equations 1a-d dependent on integrals of N_e are of the form encountered for refraction in a spherically symmetric medium. The other terms have an explicit dependence on the horizontal gradients of the electron density.

For satellite altitudes above the ionospheric layer the Equations (1a-d) can be approximated (Ref. 3) by:

Equatorial mode

$$\Delta \ell_{e,i} = \frac{\eta \sin \alpha}{\cos \lambda_0} \frac{(R_c - R_m)}{R_c \cos \phi_m} \left(\frac{\partial N_t}{r_m \partial \mu} \right) \tag{3a}$$

$$\Delta m_{e,i} = - \frac{\eta N_t r_0 r_c \sin \beta \cos \beta \cos \phi_c}{R_c r_m^2 \cos^3 \phi_m} + \eta \frac{(R_c - R_m)}{R_c} \left(\frac{\partial N_t}{r_m \partial \lambda} \right) \frac{\sin \beta}{\cos^2 \phi_m} \tag{3b}$$

Polar mode

$$\Delta \ell_{p,i} = - \frac{\eta N_t r_0 r_c \sin \alpha \cos \alpha \cos \phi_c}{R_c r_m^2 \cos^3 \phi_m} + \eta \frac{(R_c - R_m)}{R_c} \left(\frac{\partial N_t}{r_m \partial \mu} \right) \frac{\sin \alpha}{\cos^2 \phi_m} \tag{3c}$$

$$\Delta m_{p,i} = \eta \sin \beta \left(\frac{\partial N_t}{r_m \partial \lambda} \right) \frac{(R_c - R_m)}{R_c \cos \phi_m} \tag{3d}$$

where

$$r_0 \sin \phi_0 = r_m \sin \phi_m \tag{4}$$

and N_t denotes total integrated vertical columnar electron content at m and $\partial N_t / r_m \partial \lambda$ and $\partial N_t / r_m \cos \lambda_0 \partial \mu$ are the latitudinal and longitudinal gradients of N_t, respectively. The point, m, the so-called ionospheric point, is the median point for electron content along the ray path from station to satellite. Thus, the ionospheric parameters needed to calculate the refraction are N_t, its horizontal gradient components, and median altitude of electron content, $h_m = r_m - r_0$.

Ionospheric model. Although we are primarily concerned with stations of the northern hemisphere where the preponderant bulk of the tracking data was acquired we will as a matter of general interest describe an ionospheric model applicable to the southern hemisphere as well. Our model for N_t corresponds to the mean quiet ionosphere of the test period. The day-to-day fluctuations of about 20% which are a familiar feature of even the quiet conditions constitute a deviation of the model from the real medium. Strong geomagnetic disturbances lead to still wider

deviations from the mean. A commonly used index for the disturbance is K_p, the three hour planetary geomagnetic index. $K_p \leq 2$ indicates quiet conditions; $K_p \geq 3$ indicates increasing degrees of disturbance; and a daily sum $\Sigma K_p \leq 16_0$ indicates a quiet day. The general level of magnetic activity was quite low through the days of the test period (Dec. 31, 1965-Jan. 5, 1966), the daily sum being $\leq 16_0$ (Lincoln, Ref. 4). The three hour index did rise above 2 for several intervals, once reaching 5. However the generally common low activity indicates that the quiet ionosphere largely prevailed.

We construct the ionospheric model from data on N_t which are in general observed at sites remote from the Minitrack stations. There are physical models based on theoretical grounds which are useful for this purpose. Our method is, like the model for describing the world-wide behavior of f_0 F2, to consider N_t as a function of magnetic dip latitude and local time (Rishbeth, Ref. 6 and 7). Studies of observational data show the model has validity in the zone near the magnetic equator where the ionsophere is under strong geomagnetic control. The model's usefulness though decreases at the high latitudes.

The data for determining the parametric variations of N_t are based primarily on ionospheric observations during the months Dec. '65-Jan. '66 and the corresponding months of the preceding year which were also during the solar sunspot cycle minimum. In addition, N_t data for the other months of 1965 proved useful for assessing the seasonal factor.

Table 3 lists references for data mainly on diurnal variations of N_t. The measurements of Basu (Ref. 17) on latitudinal variations describe the geomagnetic anomaly, a phenomena characterized by a mid-day dip of N_t at the magnetic equator and crests to the north and south. The data of Titheridge and Smith (Ref. 21), although in a phase of higher sunspot number are used to estimate the slope of the latitudinal variations of N_t for the interval, 19°S to 55°S magnetic dip latitude.

The data from the references on the northern hemisphere for the most part show consistency in latitudinal variation. One exception is Tyagi (Ref. 15) whose daytime data on N_t is below the trend of other observers. There is also a difference between the data of Liszka (Ref. 8) and Schmelovsky (Ref. 9) even though their measurements are for a common period, the winter 1964-65, and for overlapping geographical areas.

The Minitrack data studied in this report pertain for the greater part to tracking during the nighttime ionospheric conditions with a minor fraction during the late afternoon. The local time of the observations are approximately from 1430 to 0430. Figure 4 shows N_t vs. magnetic dip latitude at select local times 1400, 1900, 2300, 0200, and 0600 which cover the tracking periods.

Horizontal gradients of N_t. For an approximate evaluation of refraction the mean latitudinal and longitudinal gradients of N_t are determined from the data in Figure 4 using the expressions

$$\text{lat. grad } N_t(\bar{\lambda}, t) = \frac{N_t(\lambda_2, t) - N_t(\lambda_1, t)}{r_m(\lambda_2 - \lambda_1)} \tag{5}$$

Table 3

References Mainly on Diurnal Variation of Total Electron Content at Various Magnetic Dip Latitudes During or Near the Solar Sunspot Minimum

Ref. No.	Location	Observational Magnetic Dip Latitude	Period
8	Sweden	70°N-78°N	Winter, '64-'65
9	Germany	62°N-74°N	Winter, '64-'65
10	Massachusetts	72°N	May-June '65
11	Urbana	68°N	June-Nov. '65
12	Boulder	65°N	Winter, '65-'66
13	Florence	58°N	June-July '65
14	Kingston	50°N	Mar.-June '65
14	Haifa	48°N	Mar.-June '65
15	Delhi	42°N	Winter, '64-'65, '65-'66
16	Hawaii	40°N	Dec. '65
17*	Calcutta	20°N-35°N	'66, '67
18	Khartoum	11°N	Winter, '64-'65
19*	Southeast Asia	39°N-28°S	'64, '65
20	Nigeria	2°N	Winter, '64-'65
14	Nairobi	29°S	Mar.-June '65
21	Rarotonga 21.2S, 200.2°E	20°S-49°S	Summer, '66-'67
22	Auckland	62°S	Dec. '65-Jan. '66
23	Sydney	64°S	Dec. '65-Jan. '66
23	Rockband	65°S	Dec. '65-Jan. '66

*Data on latitudinal variation of N_t.

and

$$\text{long. grad } N_t(\lambda, \bar{t}) = \frac{T\{N_t(\lambda, t_2) - N_t(\lambda, t_1)\}}{(t_2 - t_1)\, 2\pi r_m \cos\bar{\lambda}} \tag{6}$$

where

$$\bar{t} = \frac{t_1 + t_2}{2}, \quad \bar{\lambda} = \frac{\lambda_1 + \lambda_2}{2}$$

and t denotes local time, λ is geographic latitude, and T is the period of rotation of the earth. In applying the above formulas with reference to the data of Figure 4, the magnetic dip latitude of the tracking stations (Table 4) must be converted to geographic latitude (Cain, Ref. 24).

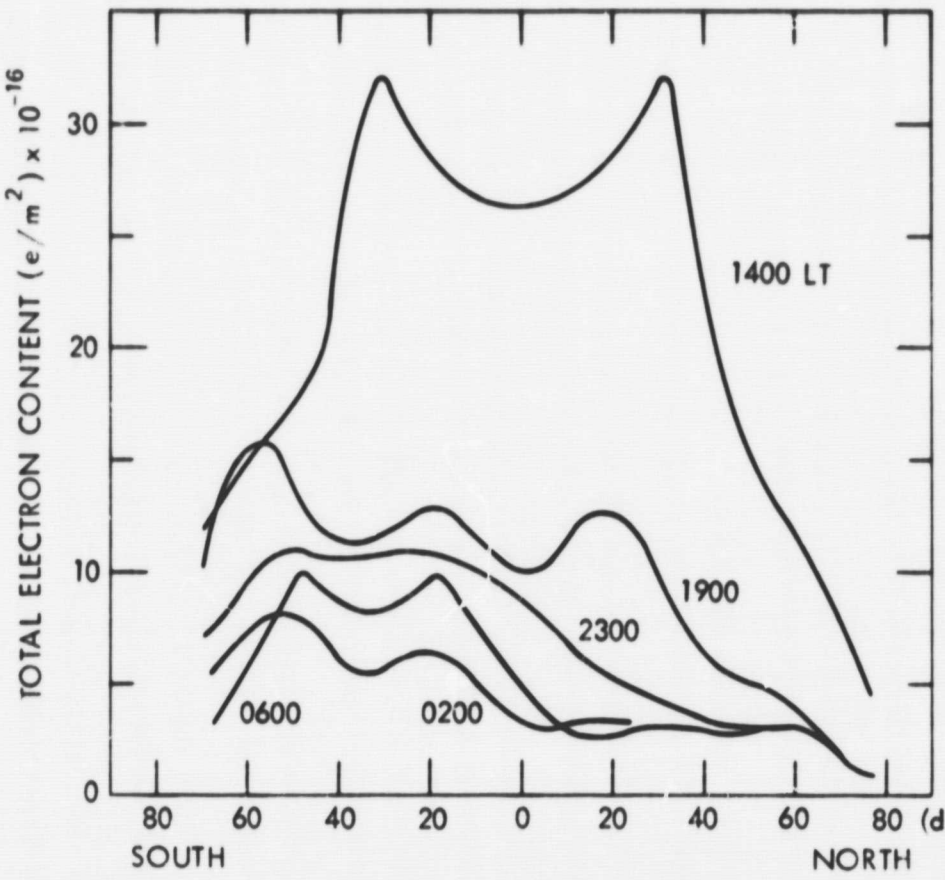

Figure 4- Total electron content vs magnetic dip latitude. Ionosphere model for Dec. 1965-Jan. 1966 at select times of the diurnal cycle.

Table 4
Tracking Station Coordinates

Tracking Station	Longitude (East)	Latitude	Magnetic Dip Latitude
College, Alaska	212°	65°N	77°N
East Grand Forks, Minn.	263°	48°N	74°N
St. John's, New Foundland	307°	48°N	72°N
Blossom Point, Maryland	283°	38°N	70°N
Winkfield, England	359°	51°N	66°N
Mojave, California	243°	35°N	60°N
Fort Myers, Florida	278°	27°N	60°N
Quito, Ecuador	281°	1°S	20°N
Lima, Peru	283°	12°S	1°N
Santiago, Chile	289°	33°S	30°S
Johannesburg, S. Africa	28°	26°S	62°S
Woomera, Australia	137°	31°S	63°S

Northern mid-latitude. Merrill and Lawrence (ML, Ref. 12) made observations on N_t for the period Oct. 1964 to Sept. 1966, showing diurnal variations and seasonal effects. The site, Boulder, is centrally located relative to northern hemisphere tracking stations: Mojave, Fort Myers, Blossom Point, East Grand Forks, St. John's, and College. The extrapolation of the measurements to these stations is through the latitudinal variations of N_t modeled in Figure 4.

ML have also measured the local latitudinal gradients of N_t at Boulder. The slope of N_t almost always decreases from south to north. Their data on normalized latitudinal gradients show considerable dispersion, especially during the winter. A nighttime gradient of two percent per degree latitude was common but some data ranged as high as 20% per degree latitude; while during the daytime it was 1% to 8% per degree latitude. We have taken as a mean for the nighttime, 12% per degree (corresponding to a latitudinal gradient of 1.1 $N_t/10^3$ km) and for the daytime, 4.5% per degree (corresponding to a latitudinal gradient of 0.41 $N_t/10^3$ km).

Longitudinal gradients of N_t have been measured by Rao (Ref. 11) from satellite signals during east-west passages at Urbana for the period June 1965 to Nov. 1965. These data follow approximately the slope of the diurnal cycle of N_t. This is in accord with the rule embodied in Equation 6 for determining longitudinal gradients from the dependence of N_t on local time.

Altitude (h_m) of the ionospheric point. Evans (Ref. 25) has investigated vertical electron density profiles at Millstone by the backscatter technique during 1964, a year of the solar sunspot minimum. From these observations we have adopted, h_m = 320 km corresponding to the nighttime ionosphere.

Ionospheric refractive noise. Ionospheric observations show large scale irregularities of N_t superimposed on a smooth background ionosphere. Rapid fluctuations in refraction due to irregularities tend to be smoothed in the tracking period of the Minitrack observations. Accordingly, to add refractive noise to residuals the horizontal scale size of the irregularities must be comparable to or larger than the arc through the irregular region traced by the tracked signal. For GEOS-I these arcs are less than 100 km. A power spectral analysis of Rao's data (Ref. 11) shows the wavelength of the irregularities to be predominantly between 200 km and 800 km. Hence these irregularities will be a source of refractive noise. Nighttime longitudinal gradients for the irregularities are $\sim 1 \times 10^{16}$ e/m^2/10^3 km. The corresponding refractive noise when averaged over elevation angles 15° to 90° amounts to $\sim 3 \times 10^{-5}$ in direction cosine. Although Rao's observations are for the summer and fall of 1965 we assume a similar level for the irregularities of the latitudinal and longitudinal gradients prevail for the following winter (Dec. '65-Jan. '66).

Tropospheric refractive noise. In the presence of the tropospheric medium (Schmid, Ref. 5) Minitrack measures, say for the ℓ direction cosine of the polar mode $\ell' = n_s \cos\alpha' = (1 + N_s \times 10^{-6}) \times \cos(\alpha + \epsilon)$ instead of the unperturbed $\ell = \cos\alpha$. Here, n_s, is the surface index of refraction; N_s the surface refractivity; and ϵ, the refraction angle of the ray path due to the troposphere. The perturbation is then to terms of the first order

$$\ell' - \ell = n_s \cos\alpha' - \cos\alpha \doteq \sin\alpha\,(N_s \times 10^{-6} \cot\alpha - \epsilon)$$

The mean behavior of ϵ can in good approximation be predicted from surface refractivity. For the standard atmosphere $N_s = 313$, (Bean et al., Ref. 27) the term on the right is 1×10^{-5} at an elevation angle of 15° and decreases with increasing elevation. Hence the tropospheric refraction bias is negligible.

The refraction of the real troposphere fluctuates about that predicted by the model. These effects are negligible at small zenith angles and are barely significant at low elevation angles. At an elevation of 45° the tropospheric refractive noise is estimated at about 1×10^{-5} and at 20° elevation about 2×10^{-5}.

RESIDUALS CORRECTED FOR IONOSPHERIC REFRACTION

The procedure for treating the raw residuals was to apply the ionospheric corrections and then to perform the linear regression analysis. Table 5 summarizes the bias parameters. Data on both corrected and uncorrected residuals are compared to show the change due to ionospheric refraction. The magnitude of the z parameters (corrected) have a range between a minimum of 1.4×10^{-5} (East Grand Forks, polar mode, ℓ) and a maximum of 27.8×10^{-5} (Mojave, polar mode, ℓ). The largest corrections of z are in the m, polar mode, the magnitude ranging between 3×10^{-5} and 7×10^{-5}. These changes are mainly attributable to the latitudinal gradients of N_s. The m, equatorial mode corrections are about 2×10^{-5}. For the ℓ data the corrections are 2×10^{-5} and less.

The k parameters have a wide range of variation. The minimum is 0.05×10^{-6} deg^{-1} (Mojave, polar, m) and the maximum is 5.12×10^{-6} deg^{-1} (Fort Myers, equatorial, m). The corrections on k are appreciable, the largest being for the polar mode, ℓ and the equatorial mode, m. The range of the large corrections is typically between 0.5×10^{-6} deg^{-1} and 1.0×10^{-6} deg^{-1}. The polar mode, m and equatorial, ℓ have only small changes in k, on the order of 0.2×10^{-6} deg^{-1} and less.

Residual noise. Although some station bias parameters were appreciably altered by the ionospheric refractive correction, the effects of the correction were to modify only to a minor degree the level of the standard deviations and the patterns of the residuals. The largest shift in st. dev. (Table VI) is only 2×10^{-5} (East Grand Forks, polar, m). We find that the st. dev. of the composite of ℓ and m data is unchanged at 8.5×10^{-5}. Individual modes still show wide departures from this average: at Mojave, equatorial, m and at East Grand Forks, equatorial, m the st. dev. are 13.5×10^{-5} and 4.9×10^{-5}, respectively. Residuals noise is shown in Figure 5 by station and mode.

The equatorial modes of Blossom Point and Mojave have observations concentrated at low elevation angles (~ 20°). Their composite st. dev. is 10.3×10^{-5} for 80 residuals. It appears then that Mintrack precision prevails to elevations approaching 15°.

Uncorrelated rms noise in the Minitrack residuals is attributable to several factors, mainly instrumental effects and atmospheric refraction. These are: (1) the limit of instrumental precision, given by the quantization step for phase difference measurement, 2×10^{-5}; (2) refractive noise due to large scale ionospheric irregularities estimated at $\sim 3 \times 10^{-5}$; (3) tropospheric refractive noise, $\sim 1.5 \times 10^{-5}$ (for elevation angles between 20° and 50°); and (4) uncorrected ionospheric

Table 5

Bias Parameters of the Linear Regression on Residuals Uncorrected and Corrected for Ionospheric Refraction

Tracking Station	Mode	Direction Cosine	$z \times 10^5$		$k\ (deg^{-1}) \times 10^6$	
			Uncorrected	Corrected	Uncorrected	Corrected
Blossom Point	Equatorial	ℓ	- 6.7	- 6.0	-1.66	-1.52
		m	- 4.0	- 1.5	4.18	3.54
	Polar	ℓ	- 7.6	- 5.6	0.83	-0.23
		m	- 4.4	1.4	-0.69	-0.85
College	Equatorial	ℓ	- 3.8	- 5.2	-5.53	-5.05
		m	9.7	15.0	1.58	0.33
E. Grand Forks	Equatorial	ℓ	7.5	8.1	1.10	1.20
		m	-3.7	- 1.5	-0.37	-0.94
	Polar	ℓ	-0.6	1.4	2.38	1.45
		m	15.5	20.4	-0.82	-0.79
Fort Myers	Equatorial	ℓ	14.6	16.4	-3.13	-3.20
		m	- 5.1	- 2.8	5.99	5.12
	Polar	ℓ	- 1.1	1.5	4.28	3.00
		m	-33.1	-26.3	0.05	-0.42
Mojave	Equatorial	ℓ	24.4	26.2	1.86	2.04
		m	- 5.8	- 1.9	2.43	1.78
	Polar	ℓ	24.9	27.8	2.59	1.55
		m	-14.2	- 7.4	0.12	-0.05
St. John's	Equatorial	ℓ	-12.6	-12.3	-0.24	-0.17
		m	1.8	4.0	3.65	2.98
	Polar	ℓ	-14.1	-12.2	3.94	3.14
		m	- 0.6	4.0	-0.18	-0.20
Winkfield	Equatorial	ℓ	9.1	9.8	-3.45	-3.34
		m	-19.6	-16.1	-0.21	-0.89

refraction due to day-to-day fluctuations of the medium, $\sim 1 \times 10^{-5}$. Combining these terms according to the rms rule gives $\sim 4 \times 10^{-5}$. At the high latitude station, College, this would be about $\sim 3 \times 10^{-5}$ due to reduced ionospheric effects. Obviously, these numbers are much affected by the leading term, the ionospheric irregularities in which there is a degree of uncertainty.

Residual noise in the time domain. The residual noise, 8.5×10^{-5}, is considerably in excess of the estimated uncorrelated rms noise, 4×10^{-5}. The difference appears to be attributable in large measure to systematic effects imbedded in the residuals and irregular perturbation effects.

Table 6

Residual Noise-Standard Deviation of the Regression Residuals

Tracking Station			Standard Deviation × 10^5							
			ℓ_e	ℓ_p	ℓ_e	ℓ_p	m_e	m_p	m_e	m_p
	Equatorial	Polar	Uncorrected		Corrected		Uncorrected		Corrected	
Blossom Point	23	17	10.2	8.1	10.1	7.6	8.7	5.0	8.5	6.1
College	15	–	8.4	–	8.4	–	5.1	–	5.2	–
East Grand Forks	17	6	7.8	11.2	7.8	10.1	5.1	10.1	4.9	12.0
Fort Myers	5	10	10.1	9.5	11.4	10.9	4.2	5.4	2.4	7.0
Mojave	17	11	9.4	9.3	9.6	8.5	13.7	8.9	13.4	8.6
St. John's	21	10	8.2	6.9	8.1	5.3	6.1	10.0	6.9	9.6
Winkfield	10	–	9.8	–	9.9	–	4.9	–	4.9	–
Composite	162		8.9		8.8		7.9		8.1	

An examination of the residual noise in the time domain gives another view of underlying bias or systematics.

Figures 6a-d show for several station modes the residual noise plotted versus time. The numbers attached to the data points indicate the day of the tracking pass. The ℓ and m residuals for a common tracking pass have the same date and time of day. We comment on the equatorial mode of Mojave (Figure 6d). In the ℓ residuals at ~0200 there is a definite positive bias while at ~ 0400 there is a reversal in the bias. These two sets are for tracking passes of consecutive orbits. The reversal in bias is pronounced. Another feature is the wide disparity between the dispersion of the ℓ and m residual pairs at ~ 0200. The five ℓ residuals have a very small dispersion, 5×10^{-5}, and the corresponding m residuals have a very large dispersion, 32×10^{-5}. It appears that the high residual noise level of this mode stems from apparent bias effects and an irregular perturbation.

The equatorial mode of East Grand Forks (Figure 6b) has one of the lowest residual noise levels in our data set. The m residuals (st. dev. = 4.9×10^{-5}) show little evidence of systematic effects. The ℓ residuals (st. dev. = 7.8×10^{-5}) do show bias effects at ~0200 and ~ 0400.

In the equatorial mode of Blossom Point (Figure 6a) the st. dev. is large but bias effects do not appear in any obvious form.

In the equatorial mode of College the residuals have systematics differing from preceding examples. Here (Figure 6e) there is a positive correlation between the ℓ and m residual pairs corresponding to a common tracking pass. In twelve of the pairs the ℓ and m residuals have a common sign, out of a total of fifteen pairs. The m residuals have a st. dev. of 5.2×10^{-5}, which while one of lowest in the data set, is still significantly above the uncorrelated rms residual estimated to be near 3×10^{-5}. This descrepancy could in the main be due to effects in the correlation between the ℓ and m residuals.

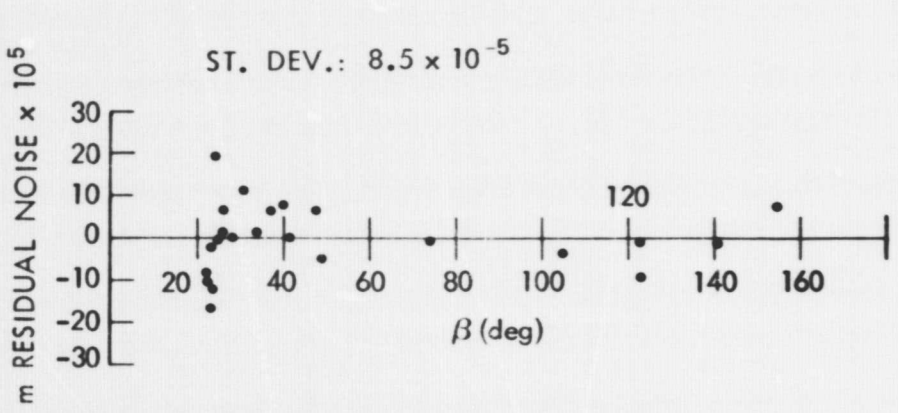

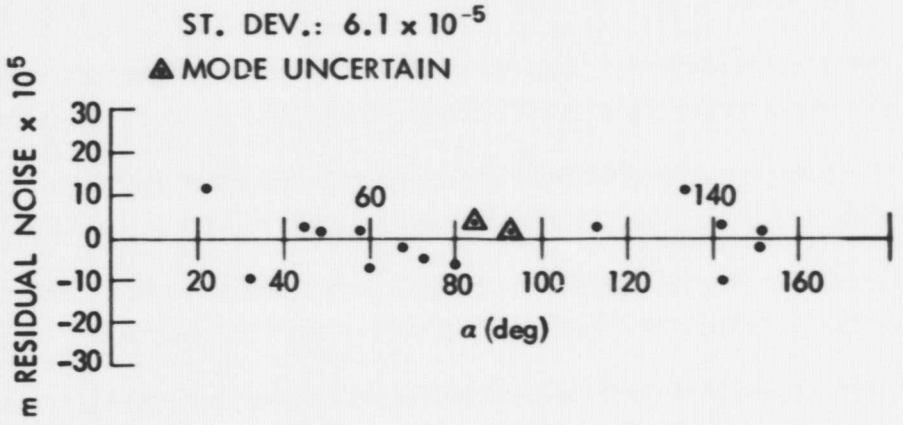

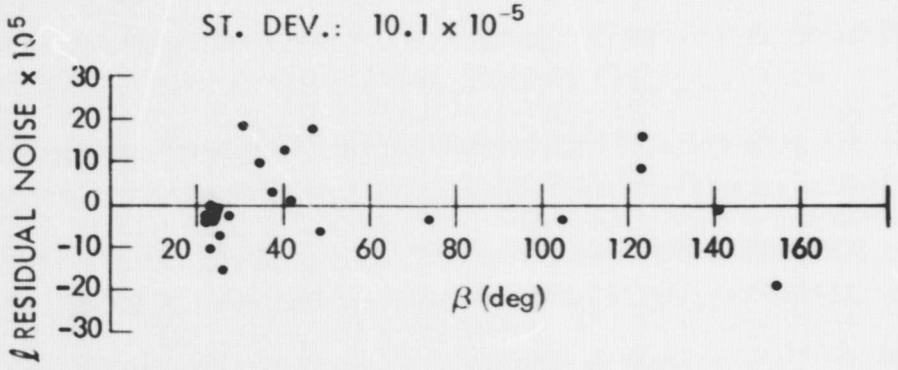

a. Blossom Point, Maryland Equatorial mode

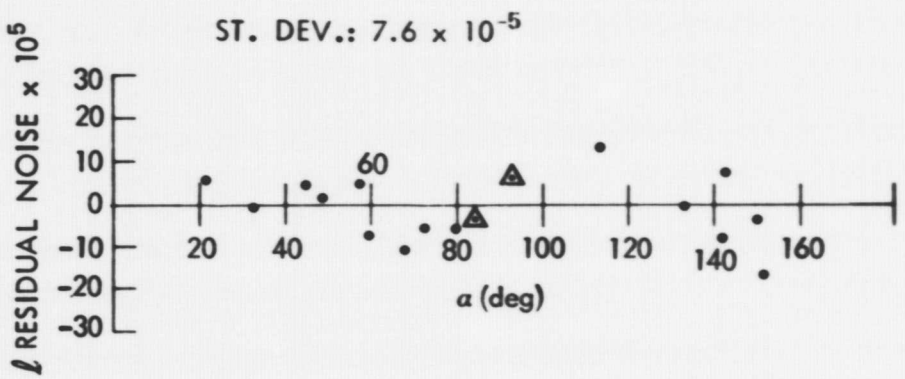

b. Blossom Point, Maryland Polar mode

Figure 5 - Direction cosine residual (corrected for ionospheric refraction and linear bias) $\times 10^5$ vs. Minitrack angle (α for the polar mode, β for the equatorial mode).

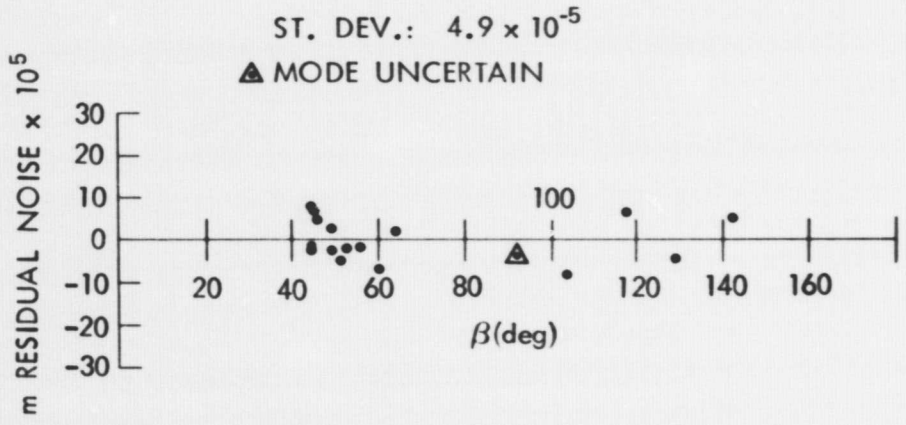

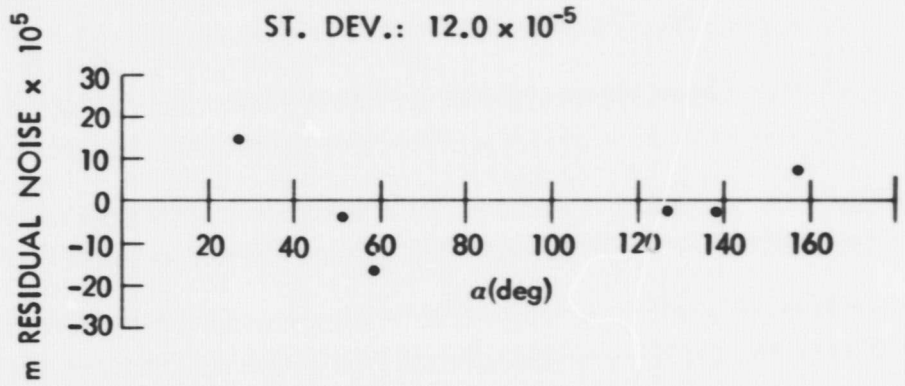

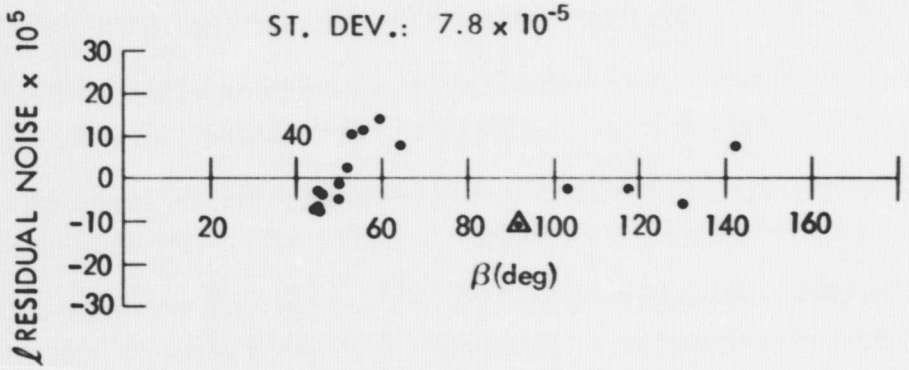

c. E. Grand Forks, Minn. Equatorial mode

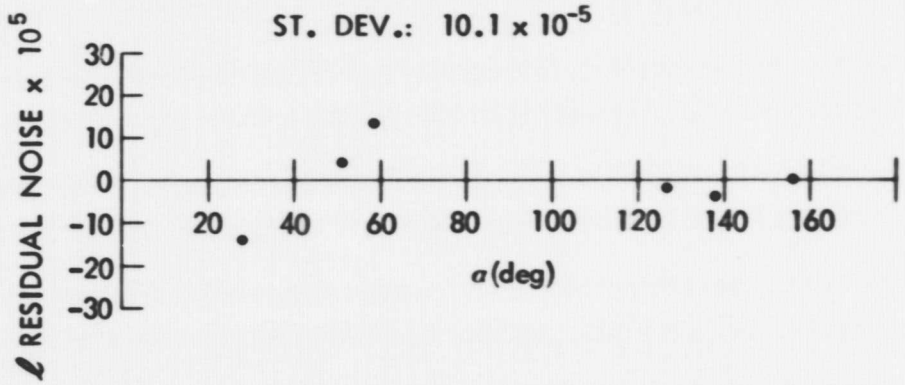

d. E. Grand Forks, Minn. Polar mode

Figure 5 - Direction cosine residual (corrected for ionospheric refraction and linear bias) $\times 10^5$ vs. Minitrack angle (α for the polar mode, β for the equatorial mode).

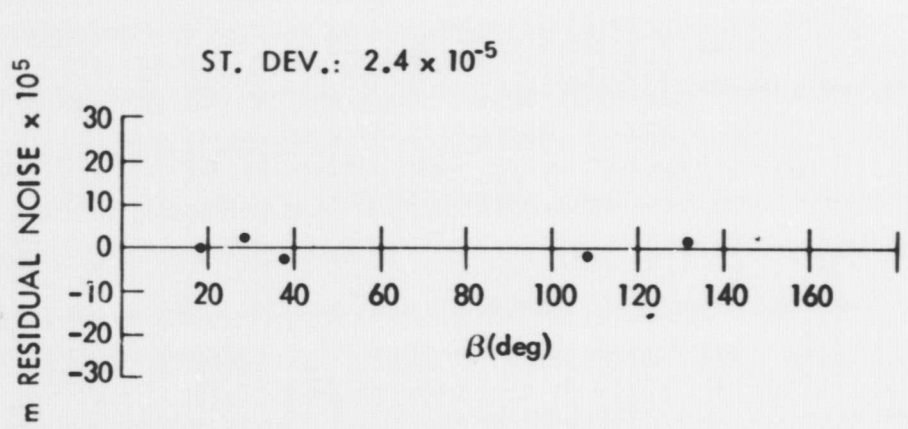

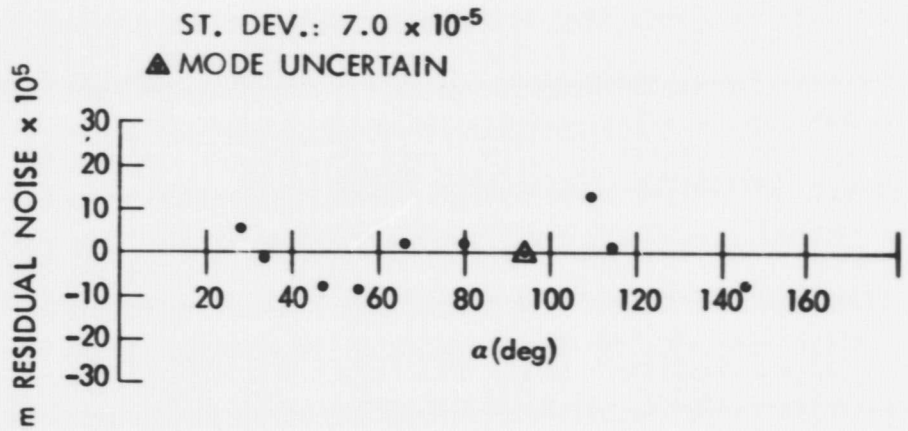

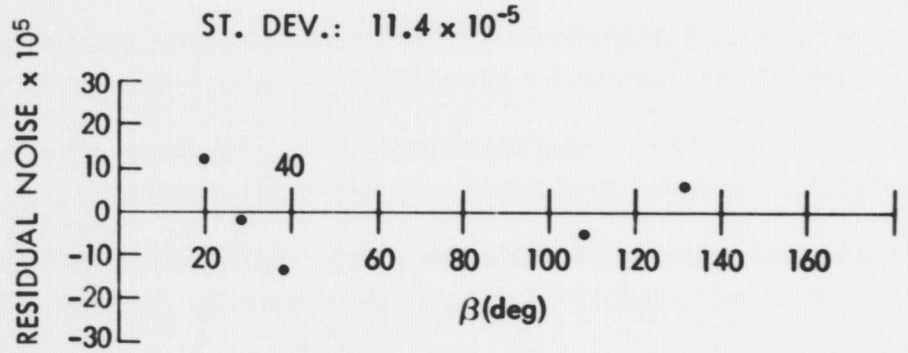

e. Fort Myers, Florida Equatorial mode

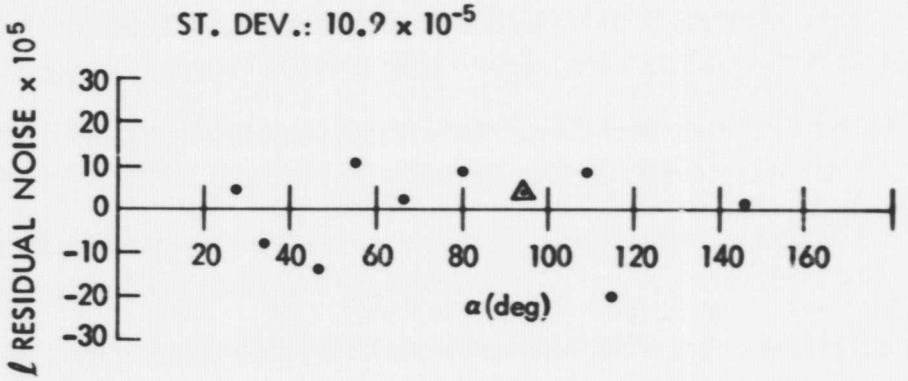

f. Fort Myers, Florida Polar mode

Figure 5 - Direction cosine residual (corrected for ionospheric refraction and linear bias) $\times 10^5$ vs. Minitrack angle (α for the polar mode, β for the equatorial mode).

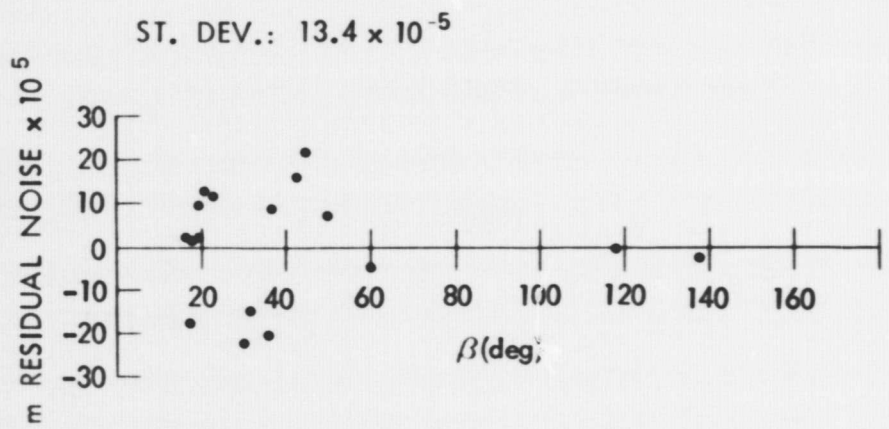

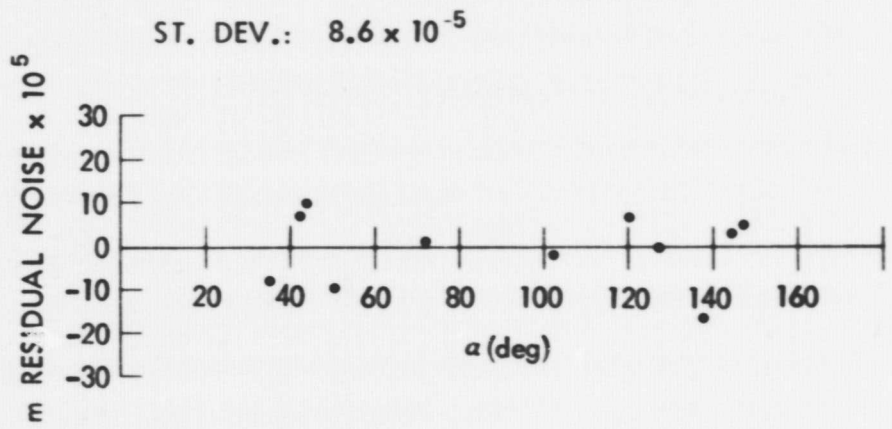

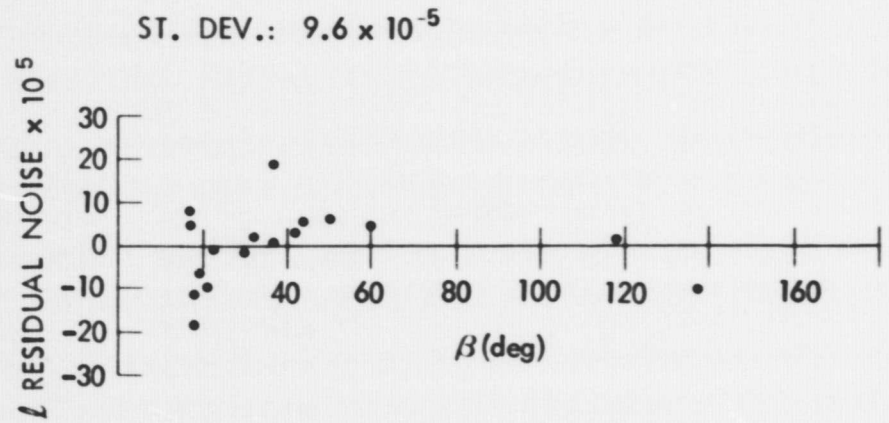

g. Mojave, California Equatorial mode

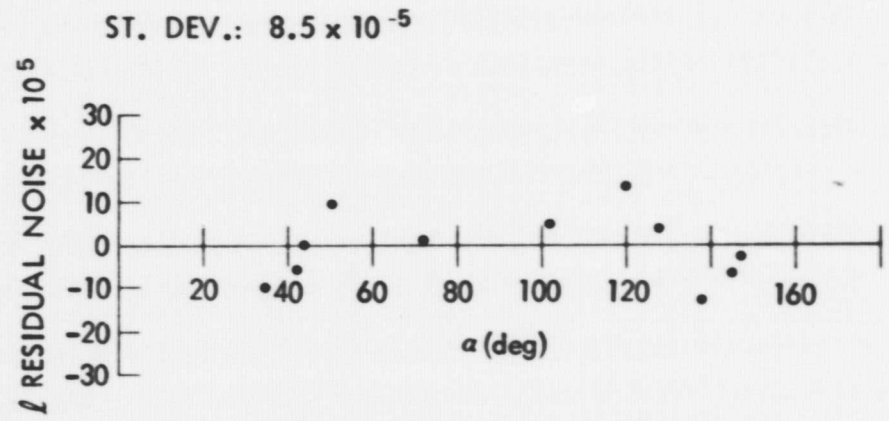

h. Mojave, California Polar mode

Figure 5 - Direction cosine residual (corrected for ionospheric refraction and linear bias) $\times 10^5$ vs. Minitrack angle (α for the polar mode, β for the equatorial mode).

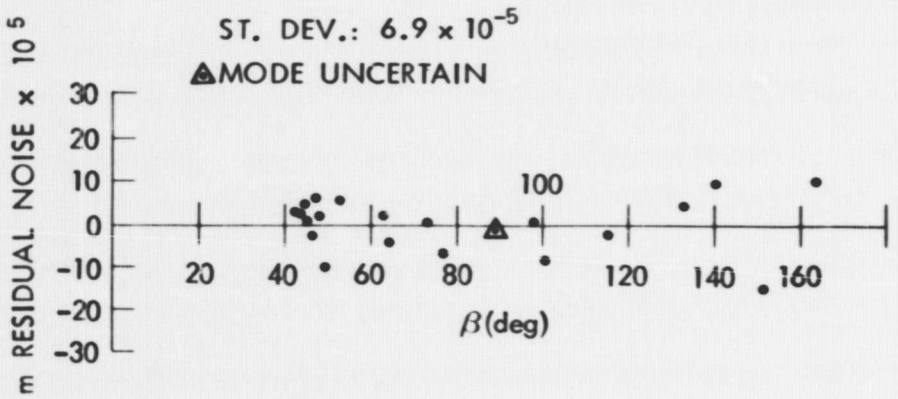

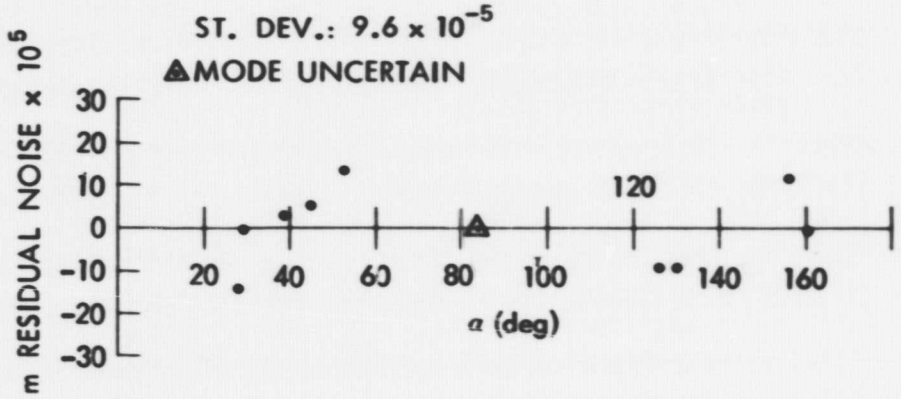

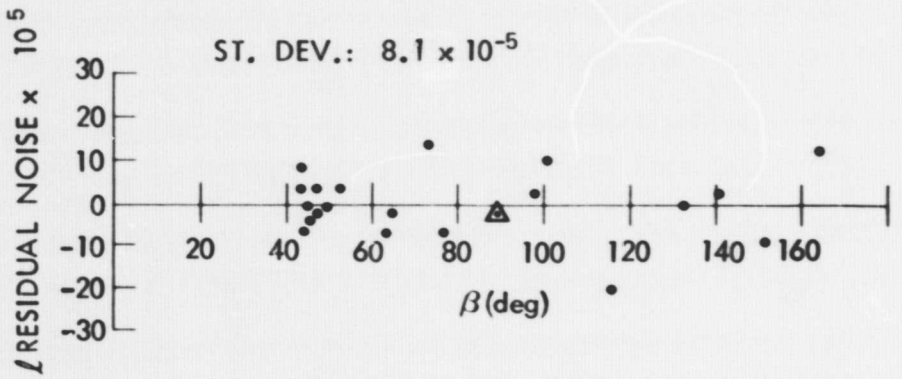

i. St. John's, Newfoundland Equatorial mode

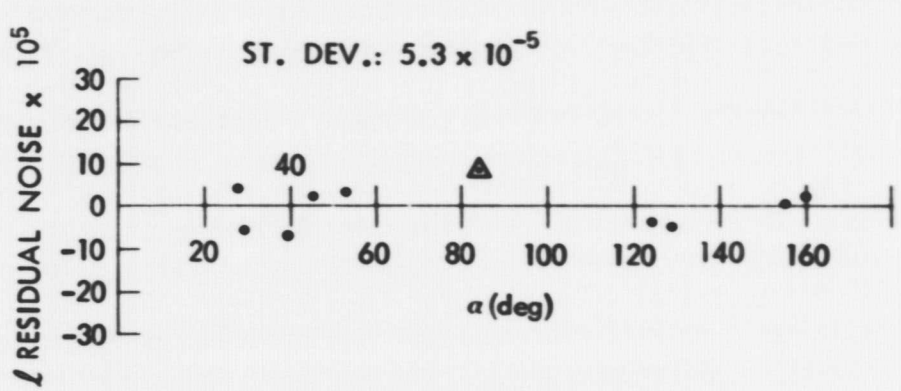

j. St. John's, Newfoundland Polar mode

Figure 5 - Direction cosine residual (corrected for ionospheric refraction and linear bias) $\times 10^5$ vs. Minitrack angle (α for the polar mode, β for the equatorial mode).

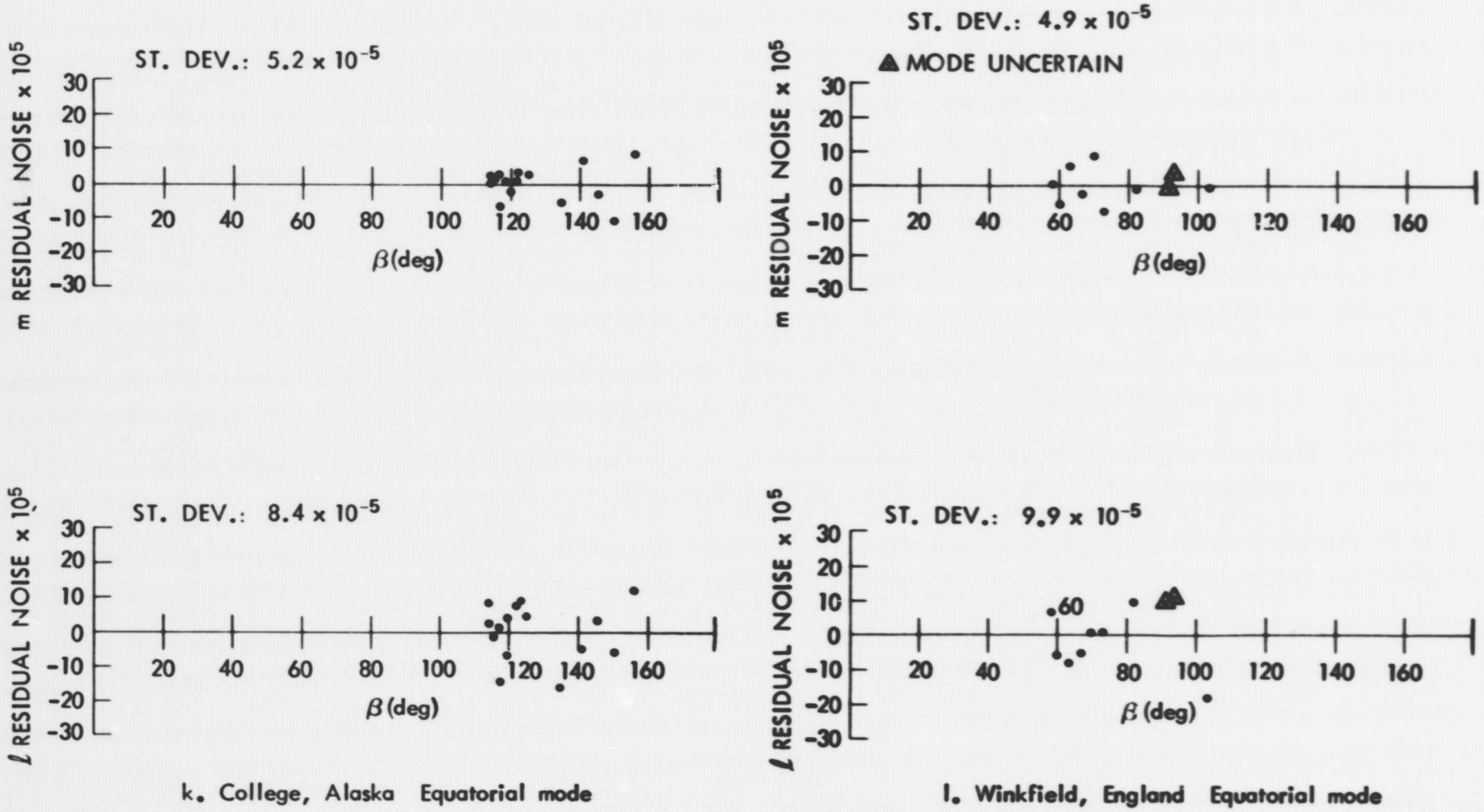

k. College, Alaska Equatorial mode

l. Winkfield, England Equatorial mode

Figure 5 - Direction cosine residual (corrected for ionospheric refraction and linear bias) $\times 10^5$ vs. Minitrack angle (α for the polar mode, β for the equatorial mode).

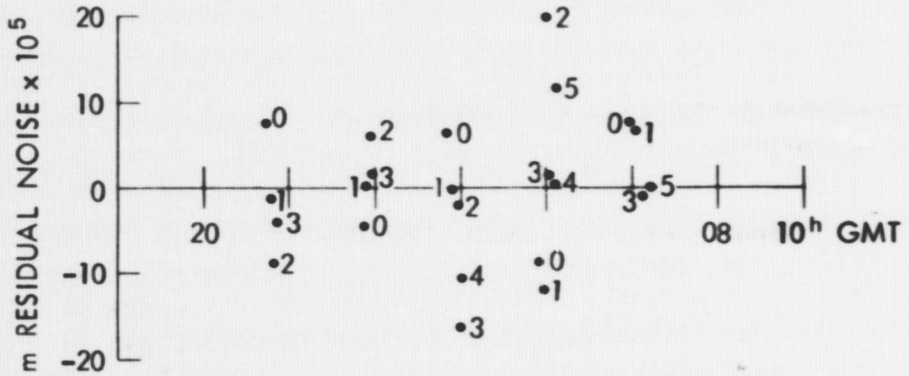

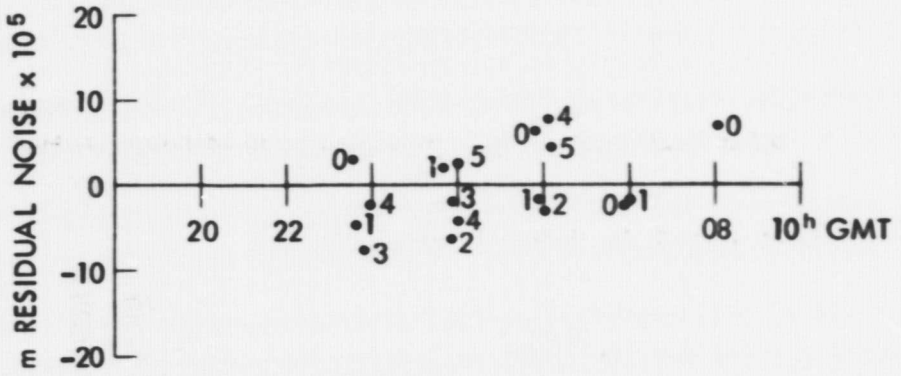

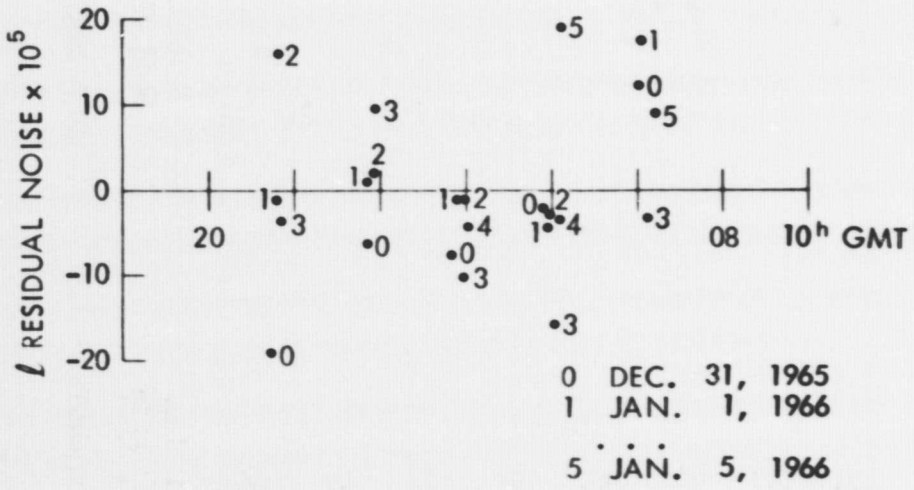

a. Blossom Point, Maryland Equatorial mode

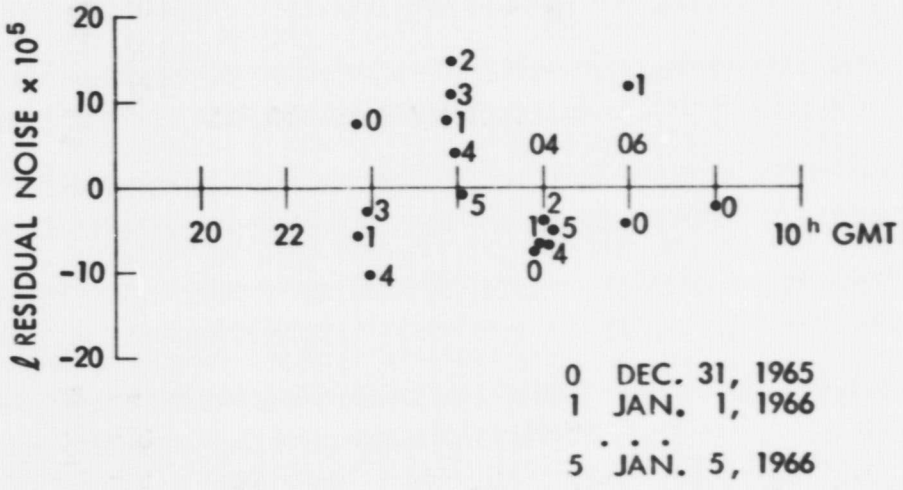

b. East Grand Forks, Minnesota Equatorial mode

Figure 6 - Direction cosine residual (corrected for ionospheric refraction and linear bias) $\times 10^5$ vs. time.

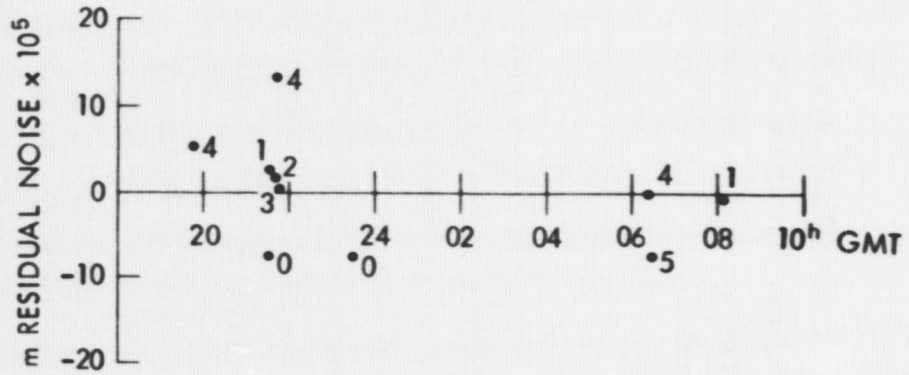

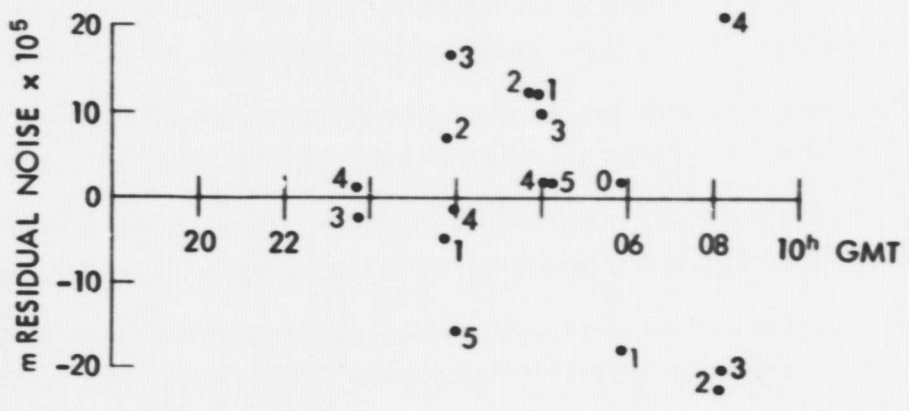

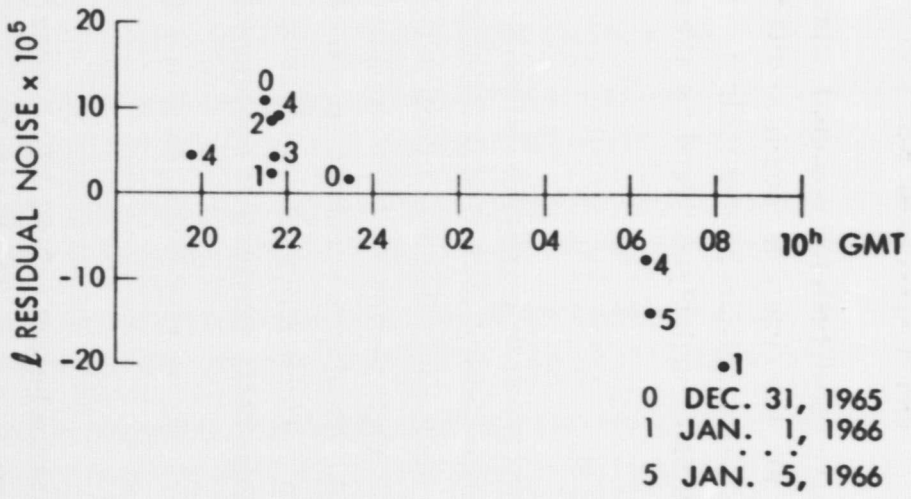

c. Fort Myers, Florida Polar mode

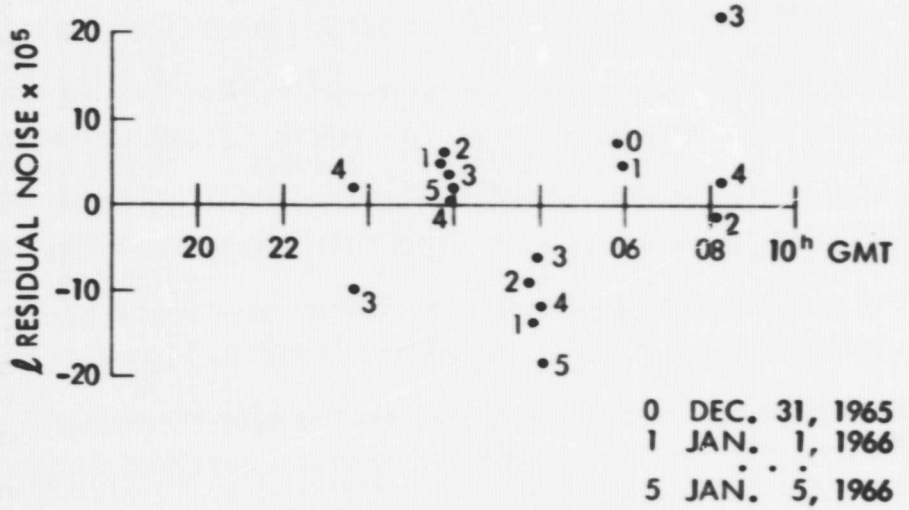

d. Mojave, California Equatorial mode

Figure 6 - Direction cosine residual (corrected for ionospheric refraction and linear bias) $\times 10^5$ vs. time.

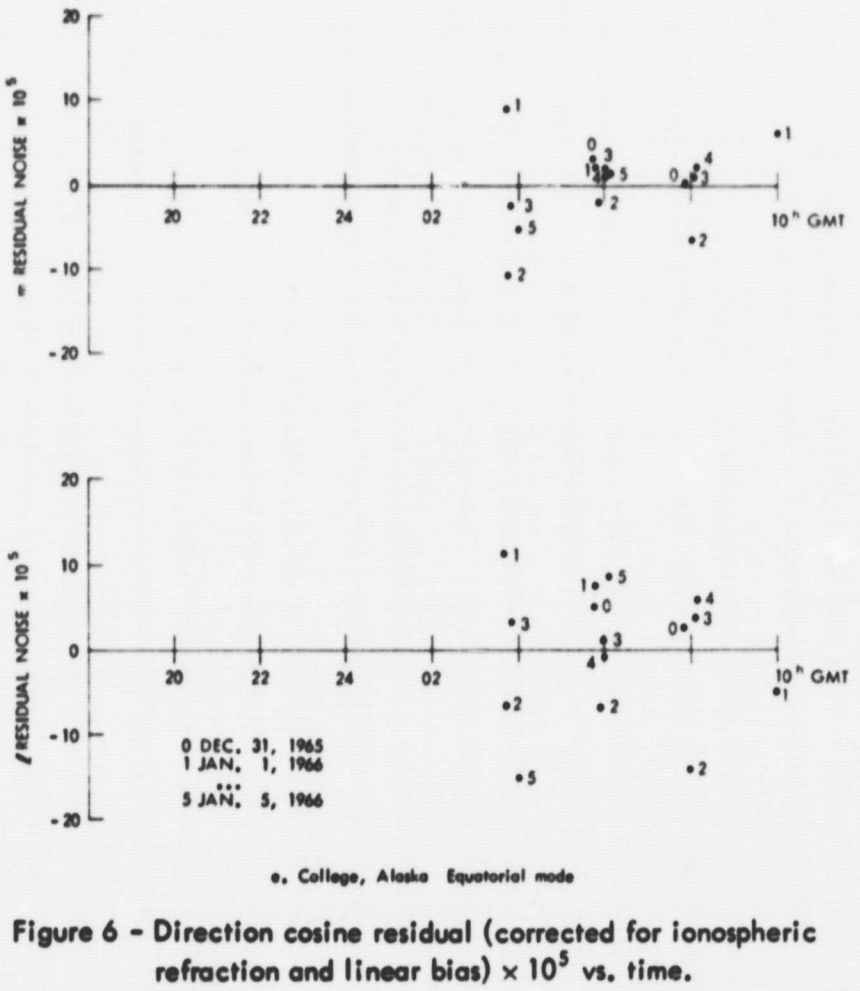

e. College, Alaska Equatorial mode

Figure 6 - Direction cosine residual (corrected for ionospheric refraction and linear bias) × 10^5 vs. time.

Systematics have now been noted both for residual noise plotted versus Minitrack angle and versus time. They possibly are the result of combined effects of regularities in the tracking observations and of tracking perturbations having their own regularities. Due to the limited data we not attempt to establish a basic underlying trend for the systematics.

CONCLUSIONS

The results of this investigation demonstrate the utility of the precisely determined reference orbit of Marsh et al. for the analysis of perturbation effects in Minitrack observations below the 10^{-4} level. A finding of the analysis is that the direction cosine measurements have a linear bias with respect to the Minitrack angle measured from the antenna beam baseline. When the test data are corrected for this bias the Minitrack accuracy appears to be maintained for observations to zenith angles approaching 75°. The residual noise of the composite data is calculated to be 8.5 × 10^{-5}. Imbedded in the residual noise are further systematic effects, the character of which remains to be clarified.

ACKNOWLEDGMENTS

The author gratefully acknowledges valued discussions with C. E. Doll, Jr., J. Berbert, F. Lerch, J. G. Marsh, Dr. J. Ramasastry, and W. M. Rice. For the programmed computations the author is indebted to J. F. Cook, C. W. Murray, and H. P. Swartwood, Jr.

REFERENCES

1. Marsh, J. G. and Doll, C. E., Sandifer, R. J and Taylor, W. A., "Intercomparison of the Minitrack and Optical Tracking Networks U[illegible]g GEOS-I Long Arc Orbital Solutions," NASA TN D-5337, Feb. 1970.

2. "Geodetic Parameters for a 1966 Smithsonian Institution Standard Earth," Vol. I, ed. by C. A. Lundguist and G. Veis, SAO Special Report No. 200, 1966.

3. Rosenbaum, B., "Ionospheric Perturbations on STADAN VHF Tracking Accuracy," GSFC, X-551-69-403, Sept. 1969.

4. Lincoln, J. Virginia, "Geomagnetic and Solar Data," J. Geophys. Res., 71, 2411-2417 (1966); 71, 2862-2864 (1966); 72, 2981-2984.

5. Schmid, P. E., "NASA Minitrack Interferometer Refraction Corrections," GSFC, X-551-69-434, Oct. 1969.

6. Rishbeth, H., "A Review of Ionospehric F Region Theory," Proc. IEEE, 55, 16-35 (1967).

7. Rishbeth, H., "On Explaining the Behavior of the Ionospheric F Region," Rev. Geophys., 6, 33-71 (1968).

8. Liszka, L., "Latitudinal and Diurnal Variations of Ionospheric Electron Content near the Auroral Zone in Winter," Radio Sci. (New Ser.), 1, 1135-1137 (1966).

9. Schmelovsky, K. H., "The Outer Ionosphere," Space Science Reviews, 8, 74-91 (1968).

10. Klobuchar, J. A. and Whitney, H. E., "Middle Latitude Ionospheric Total Electron Content: Summer 1965," Radio Sci. (New Ser.), 1149-1154 (1966).

11. Rao, N. N., "Ionospheric Electron Content and Irregularities Deduced from BE-C Satellite Transmission," J. Geophys. Res., 72, 2929-2942 (1967).

12. Merrill, R. G. and Lawrence, R. S., "Ionospheric Electron Content at Midlatitude near the Minimum of the Solar Cycle," J. Geophys. Res., 74, 4661-4666 (1969).

13. Checcacci, P. F., "Ionospheric Measurements by Means of the Early Bird Geostationary Satellite," Radio Sci., 1 (New Ser.), 1154-1158 (1966).

14. Joint Satellite Studies Group, "Ionospheric Electron Content and Scintillation Studies at Widely Spaced Low Latitude Stations," Planet. Space Sci., 16, 1277-1289 (1968).

15. Tyagi, T. R., "Satellite Beacon Studies of the Ionosphere over Delhi," Sci. Rept. 34, National Physical Laboratory, New Delhi, India, Aug. 1, 1967.

16. Yuen, P. C. and Roelofs, T. H., "Seasonal Variations in Ionospheric Total Electron Content," J. Atmosph. Terr. Phys., 29, 321-326 (1967).

17. Basu, S. and Das Gupta, A., "Latitude Variation of Electron Content in the Equatorial Region under Magnetically Quiet and Active Conditions," J. Geophys. Res., 73, 5599-5602 (1968).

18. Jayendran, A. and O'brien, P. A., "Measurement of Ionospheric Electron Content over Khartoum," J. Atmosph. Terr. Phys., 31, 555-562 (1969).

19. Rufenach, G. L., Nimit, V. T., and Leo, R. E., "Faraday Rotation Measurements of Electron Content near the Magnetic Equator," J. Geophys. Res., 73, 2459-2468 (1968).

20. Skinner, N. J., "Measurements of Total Electron Content near the Magnetic Equator," Planet. Space Sci., 14, 1123-1129 (1966).

21. Titheridge, J. E., and Smith, W. D., "The Electron Content of the Low Latitude Ionosphere," Planet. Space Sci., 17, 1967-1976 (1969).

22. Titheridge, J. E., "Continuous Records of the Total Electron Content of the Ionosphere," J. Atmosph. Terr. Phys., 28, 1135-1150 (1966).

23. Nelson, G. G., "Total Ionospheric Electron Content at Middle Latitudes during Sunspot Minimum," J. Atmosph. Terr. Phys., 30, 513-526 (1968).

24. Cain, J. C., "Automatic Mapping of the Geomagnetic Field," J. Geophys. Res., 68, 4689-4696 (1963).

25. Evans, J. V., "Midlatitude F-Region Densities and Temperatures at Sunspot Minimum," Planet. Space Sci., 15, 1387-1405 (1967).

26. Berbert, J. H., Oosterhout, J. D., Engels, P. D., and Habib, J. E., "Minitrack Calibration System," Phot. Sci. Eng., 7, 78-83 (1963).

27. Bean, B. R., and Thayer, G. D., "CRPL Exponential Reference Atmosphere," National Bureau of Standards, Monograph No. 4, 1966.